*J. Paleont.*, 64(5), 1990, pp. 700–724

0022-3360/90/0064-0700$03.00

# A NEW FAMILY OF TREPOSTOME BRYOZOANS FROM THE ORDOVICIAN SIMPSON GROUP OF OKLAHOMA

MARCUS M. KEY, JR.
Department of Geology, Dickinson College, Carlisle, Pennsylvania 17013

ABSTRACT—A new family, Bimuroporidae, is proposed for a clade of Ordovician trepostome bryozoans. The family is united by several characteristics, including a zooidal ontogenetic progression from mesozooid to autozooid and an integrate wall structure. Discriminant and cladistic analyses of colonies from the Ordovician Simpson Group outcropping in the Arbuckle Mountains and Criner Hills of south-central Oklahoma permit the recognition of eight species belonging to this family. Four species assigned to the new genus *Bimuropora* are described: *B. dubia* (Loeblich), *B. pollaphragmata* n. sp., *B. conferta* (Coryell), and *B. winchelli* (Ulrich), as well as four species assigned to the genus *Champlainopora* Ross: *C. chazyensis* (Ross), *C. ramusculus* n. sp., *C. pachymura* (Loeblich), and *C. arbucklensis* n. sp.

## INTRODUCTION

RECONSTRUCTING the history of life and understanding its causal evolutionary processes requires phylogenetic classifications. Many previous classifications have been largely based on phenetic similarity with no regard to phylogenetic relationships. A phylogenetic approach was adopted in this study using cladistic methodology. Traditional bryozoan taxonomic characters were used as well as characters associated with growth pattern, such as zooidal arrangement, budding pattern, and zooidal ontogeny.

This study involved the Simpson Group fauna, which is exposed in the Arbuckle Mountains and Criner Hills of south-central Oklahoma and in the Wichita Mountains of southwest Oklahoma. Analysis concentrated on exposures in the Arbuckle Mountains and Criner Hills (Figure 1) where outcrops of the Simpson Group have their greatest thicknesses and are relatively complete. The Simpson Group was deposited during the Middle Ordovician and consists of five formations: Joins, Oil Creek, McLish, Tulip Creek, and Bromide.

Deposition occurred in the subsiding Southern Oklahoma Aulacogen Basin. During all of Middle Ordovician time, this basin remained a tectonically negative area (Ross, 1976). Thus, the Simpson Group provides one of the few complete records of Middle Ordovician deposition on the North America Platform (Cooper, 1956; Ross et al., 1982). Its bryozoans are generally older (based on conodont biostratigraphy of Ross et al., 1982) than those in adjacent basins and very few of the eight ingroup species occur in other basins. The geographic, stratigraphic, and phylogenetic relationships of all of these species are discussed under Systematic Paleontology.

Description of the Simpson Group bryozoan fauna began with Decker and Merritt (1931) who listed 24 species. Loeblich (1942) described 31 species, while Merida and Boardman (1967) listed four species. Finally, Farmer (1975) described three more species.

Five stratigraphic sections were measured in this study (Figures 1 and 2). These sections include the upper three Simpson Group formations (McLish, Tulip Creek, and Bromide). They collectively represent about 15 million years of deposition during the Middle Ordovician Chazyan, Blackriveran, and Rocklandian Stages (Figure 3; Ross et al., 1982). The bryozoans studied in this report were not found in the Joins and Oil Creek Formations.

USNM collection localities are as follows. Section 1: 2130A–F, Tulip Creek Formation; 2130G, H, Bromide Formation; NW¼, NE¼, sec. 16, T5S, R1E, 7.5′ Ardmore West and Overbrook quadrangles. Section 2: 2132A–Y, Bromide Formation; SE¼, NE¼, sec. 17, T2S, R1W, 7.5′ Fox NE quadrangle. Section 3: 2114A–G and 38979, McLish Formation; 2115A–K, Tulip Creek Formation; 2116A–L and 38971–38978, Bromide Formation; S½, SE¼, sec. 24 and NE¼, sec. 25, T2S, R1E, 7.5′ Springer quadrangle. Section 4: 2129A–P, McLish Formation; 2128A–E, Tulip Creek Formation; 2127A–Q, Bromide For-

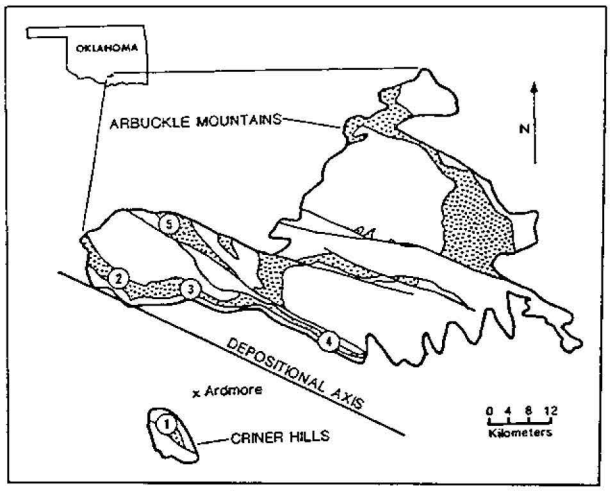


FIGURE 1—Geologic map of the Arbuckle Mountains and Criner Hills showing locations of measured and sampled stratigraphic sections. Stippling indicates Simpson Group outcrops. Redrawn from Sprinkle (1982, fig. 77).

mation; NW¼, sec. 27, T3S, R4E, 7.5′ Nebo and Troy quadrangles. Section 5: 2153A–Z, McLish Formation; 2153AA–FF and 2154A–I, Tulip Creek Formation; 2155A–Z and AA–FF, Bromide Formation; SW¼, sec. 15, T1S, R1E, 7.5′ Turner Falls quadrangle.

## MATERIALS AND METHODS

This study utilized collections of bulk material from the Simpson Group collected by R. S. Boardman in 1961 and 1962, by Boardman and G. T. Farmer, Jr. in 1963, and by Boardman and J.E. Merida in 1966. The author collected more material in 1987 to fill in the stratigraphic gaps in these existing collections. All of this bulk material is housed in the U.S. National Museum of Natural History, Bryozoa Stenolaemata General Collection.

Prior to this study, 105 colonies belonging to the ingroup had been sectioned by Boardman, Farmer, Loeblich, and Merida. To these the author added another 309 colonies, bringing the total number available for study to 414. All thin sections, acetate peels, and colony remnants are housed in the U.S. National Museum of Natural History, Paleozoic Bryozoa Stenolaemate thin section collection.

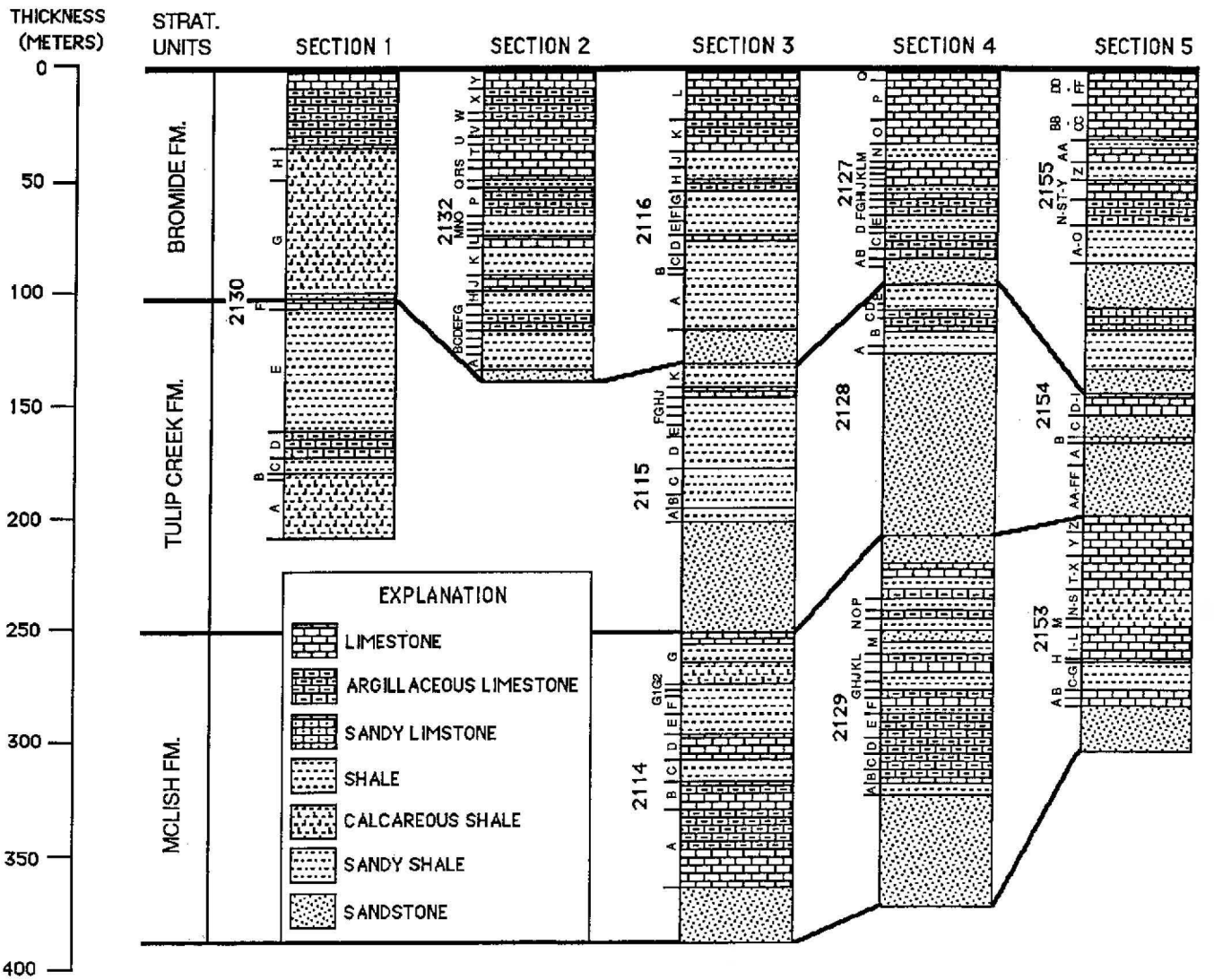


FIGURE 2—Measured stratigraphic sections showing positions of collections. See Figure 1 for locations of sections.

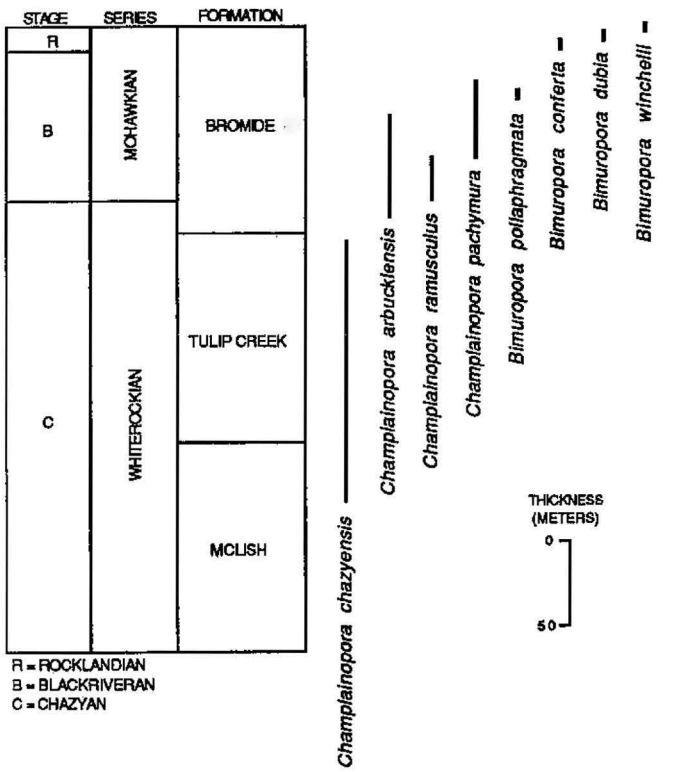


FIGURE 3—Middle Ordovician Simpson Group stratigraphic chart showing ranges of species. Modified from Ross et al. (1982).

Data were collected using transmitted light microscopy, thin-section projection, and microcomputer-based video image digitizing. Using repeatability experiments, measurement error was calculated to be 3.8 percent.

## SPECIES RECOGNITION

Fifty-five characters were analyzed in this study (Appendix 1): 40 multistate characters and 15 quantitative characters. Three of the multistate characters (4, 8, and 9) were quantitative characters that were converted into multistate characters using arbitrary gap coding. This was done by choosing distinctive breaks in the distribution of the characters' values. Six of the 15 quantitative characters (41–43, 46, 48, and 49) are measured characters, three are traditional, calculated characters (44, 45, 47), and the remaining six are counted characters. In this study, measurements and counts were replicated within each colony. As a result, counted characters vary continuously, like measured characters.

The 40 multistate characters were scored on the 414 colonies, including type-specimen colonies from previously described Middle Ordovician species that were morphologically similar to the ingroup species. Character states were coded 1, 2, 3, etc. There is no association between the character state number and the degree of primitiveness. The possible states for each character are listed in Appendix 1.

The colonies were then qualitatively grouped into eight species using the 40 multistate characters (character states of the eight species are listed in Appendix 2). The coded type-specimens from previously described Middle Ordovician species that had no representatives in the samples were dropped from the remaining analyses. The 15 quantitative characters were then measured, counted, or calculated on 131 of the 414 colonies that were most complete. An average of 16 colonies (range 13 to 25) from each of the eight species was measured. The 131 colonies included type-specimens from previously described Middle Ordovician species that were found in the Simpson Group. Each quantitative character was measured up to 10 times per colony, and the qualitative species groupings were then statistically checked with this separate set of quantitative characters. This analysis is described under Discriminant Analysis.

Most of the characters analyzed in this study are traditional bryozoan taxonomic characters. There are several characters that are relatively new to bryozoan taxonomy and these warrant mention here. These characters can be grouped into two areas: 1) hard-part characters that reflect the morphology of soft-part characters and 2) growth-pattern characters.

Bryozoologists have demonstrated a correlation between the soft parts and hard parts of living tubuliporates and Paleozoic trepostomes (McKinney and Boardman, 1985; Schafer, 1985; Winston, 1981). These studies suggest that some information on soft-part morphology is discernible in the hard parts. For example, McKinney and Boardman (1985) have shown that living-chamber diameter (character 47) is correlated with mouth level, tentacle-sheath diameter, and number of tentacles. Even though this study is based solely on hard parts, association of some soft parts is implied. It has also been proposed that the biology of Paleozoic trepostomes was similar to the biology of living tubuliporates (Boardman and McKinney, 1985). This permits the analysis of hard-part characters in their presumed biologic context. For example, autozooecial living chamber cross-sectional area (character 46) and living chamber depth (character 48) are measures of hard-part characters. These two characters are used in the systematic descriptions to calculate living chamber volume, which is related to polypide size. Thus, from hard-part characters, information on soft-part morphology can be inferred.

Growth-pattern characters (characters 5–10 in Appendix 1) refer to the growth pattern of the zooids within the colony and include budding pattern, zooidal arrangement, occurrence of long axial zooecia, number of diaphragms per mm in early zooidal ontogeny, length of the mesozooidal stage in early zooidal ontogeny, and occurrence of remnant growing tips in the endozone. The idea to include these characters came from the pioneering work by McKinney (1977) on budding pattern.

These characters were generally very stable. Some did not vary even at the family level. These characters were important in arranging the species into higher taxa and are discussed under Phylogeny Reconstruction. All species in this study exhibited an interzooidal budding pattern as opposed to the outgroup species having an intrazooidal budding pattern. The zooidal arrangement varied from *Bimuropora* with a disordered arrangement to *Champlainopora* and the outgroup with an ordered arrangement. Those species with an ordered zooidal arrangement had long, large, axial zooids. The family Bimuroporidae is also united by the presence of remnant growing tips in in the endozone and zooidal diaphragms immediately following budding in early zooidal ontogeny. This latter characteristic reflects an ontogenetic transformation in most zooids from mesozooid to autozooid.

## DISCRIMINANT ANALYSIS

The qualitative assignment of colonies into species was checked with the separate set of quantitative characters using discriminant analysis. One of the 15 quantitative characters (characters 41–55 in Appendix 1) was not utilized. Autozooidal living chamber cross-sectional diameter (character 47) was not used because this character is better represented by autozooidal living chamber cross-sectional area (character 46), which was includ-

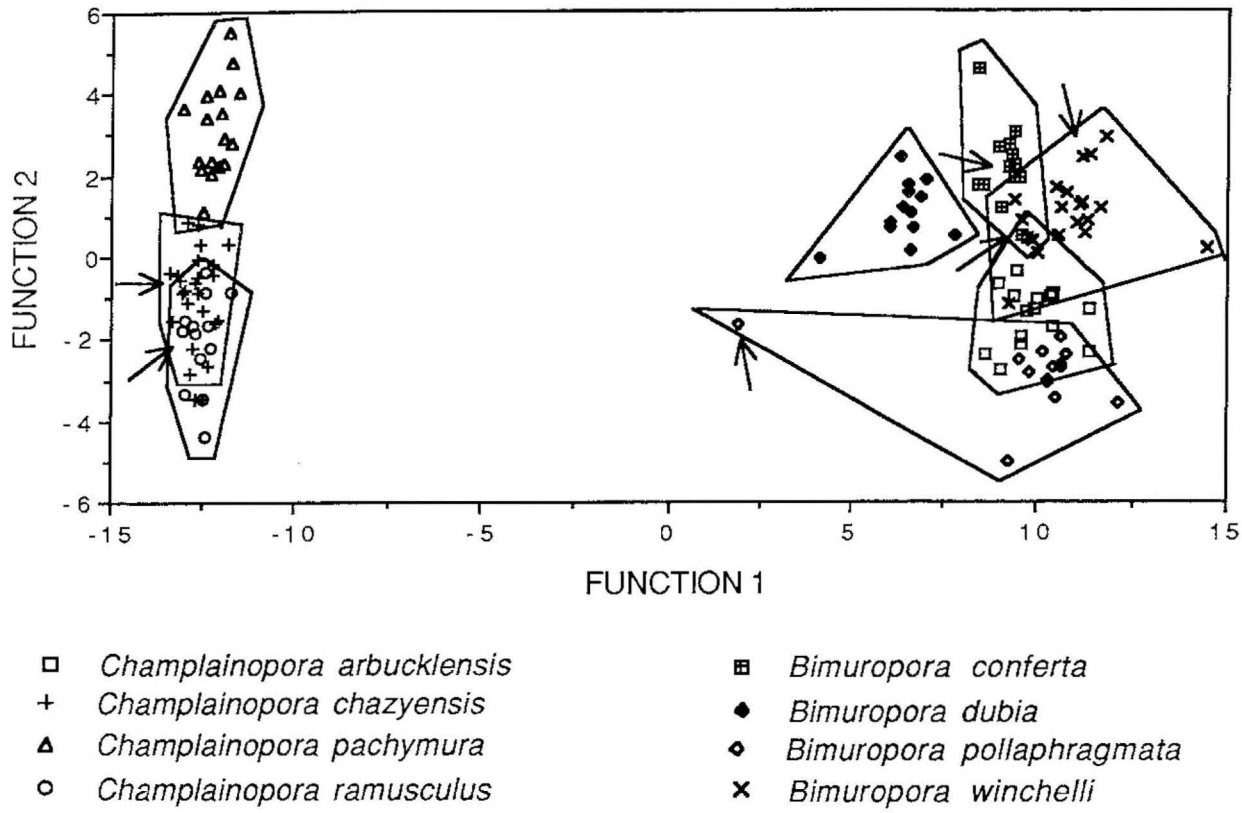


FIGURE 4—Distribution of the 131 colonies in the first two dimensions of discriminant space. Arrows refer to misassigned colonies.

ed. Character 47 was calculated and reported so these species could be compared with previously described species using this character. This character has been reported in previous trepostome species descriptions. This left 14 quantitative characters. The data consisted of these 14 characters measured on 131 colonies belonging to eight species. Each colony value was an average of up to 10 replicates within each colony. On some colonies that were small, fewer than 10 replicates were measured. Colony means were utilized to minimize the effect of nonheritable variation resulting from measurement error, varying depths and orientations of sections, and any astogenetic, ontogenetic, polymorphic, and microenvironmental variation.

The randomness of data collection was ensured by the random selection of colonies and zooids during slabbing of the bulk material. Variances among characters and species were normalized by transforming the data into natural logarithms. This required adding 1.0 to all the values of three characters (51, 54, 55) prior to transformation because of 0.0 values.

Discriminant analysis requires that there be no missing values in the data matrix. Initially, this was not the case. This problem was solved using two methods whose results were then compared. The first solution involved substituting species means for missing colony mean values. The second solution involved first dropping out the character with the most missing values and then dropping out the colonies with missing values for any of the remaining characters.

Discriminant analysis was performed using the statistical software package SPSS/PC+ (SPSS, 1988). The maximum number of discriminating functions is the lesser of either the number of characters (i.e., 14 in the first analysis and 13 in the second analysis) or one fewer than the number of species (i.e., $8 - 1 = 7$). Thus, the maximum number of functions in both analyses was seven. This was further reduced by eliminating those functions that did not significantly contribute to the discrimination of species at $P = 0.05$.

The first analysis (substituting species means for missing values) used a natural log transformed matrix of 14 characters and 131 colonies belonging to eight species. Discriminant analysis was able to significantly distinguish all eight species at $P = 0.0001$ (Table 1). With six discriminant functions (Table 2), 125 of the 131 colonies (95.4%) were correctly assigned to their species. The results from this analysis (Table 2) show that the first discriminant function explained 94.03 percent of the variance. Character 55 (number of acanthostyles per mm$^2$) loaded heavily on this function (Table 3). The second discriminant function explained another 3.00 percent of the variance (Table 2). Characters 46 (autozooecial living chamber cross-sectional area), 44 (branch diameter), and 42 (endozone diameter) loaded heavily on this function (Table 3). Therefore, a plot of function 1 vs. function 2 (Figure 4) encompasses 97.03 percent of the variance and mainly separates the colonies based on characters 55, 46, 44, and 42. Figure 4 shows the distribution of the 131 colonies in the first two of the total six dimensions of discriminant space.

The second analysis first dropped the character with the most missing values (53: number of diaphragms per mm in mesozooids) and second dropped the colonies with any remaining missing values. This resulted in a matrix of 13 characters and 51 colonies belonging to eight species. The data were natural log transformed as in the first analysis. Discriminant analysis

TABLE 1—Mahalanobis Distance matrix from the analysis using 131 colonies and 14 quantitative characters. Letters refer to species: D = *Bimuropora dubia*; L = *B. pollaphragmata*; C = *B. conferta*; W = *B. winchelli*; Z = *Champlainopora chazyensis*; R = *C. ramusculus*; P = *C. pachymura*; A = *C. arbucklensis*. * Indicates species are indistinguishable at $P = 0.05$.

| | D | L | C | W | Z | R | P | A |
|---|---|---|---|---|---|---|---|---|
| D | 0 | | | | | | | |
| L | 21 | 0 | | | | | | |
| C | 10 | 28 | 0 | | | | | |
| W | 18 | 19 | 9 | 0 | | | | |
| Z | 331 | 481 | 438 | 629 | 0 | | | |
| R | 264 | 370 | 342 | 474 | 13 | 0 | | |
| P | 272 | 415 | 358 | 502 | 22 | 33 | 0 | |
| A | 24 | 20 | 26 | 15 | 520 | 410 | 441 | 0 |

was able to significantly distinguish all but one pair of species at $P = 0.016$. *Bimuropora dubia* and *B. winchelli* were not distinguishable ($P = 0.06$). And 98.0 percent of the colonies were correctly assigned to their species.

Most of the misassigned colonies belonged to species of *Bimuropora*. This is a reflection of the phenetic similarity of these species. The misassignment of these colonies was commonly due to an outlier value in a single character. The assignment of a colony should not be made on the basis of one character. The polythetic approach (sensu Boardman et al., 1970) using the 40 qualitative characters is stronger. For this reason the qualitative assignments were given weight over these few quantitative misassignments.

In the second analysis, character 53 (number of diaphragms per mm in mesozooids) was dropped. This undoubtedly affected the results because the second analysis was unable to distinguish one pair of species. Dropping out characters and colonies can introduce a bias into the analysis. This can result if the colonies that are dropped are missing values because of extreme values for certain characters. Fortunately, the results from the two analyses are similar enough to suggest this potential bias was insignificant.

The analysis using 131 colonies discriminated species more successfully than the analysis using 51 colonies. This was expected for three reasons. First, the analysis using 131 colonies substituted species means for missing values, which reduced intraspecific variation and made it easier to discriminate between species. Second, the analysis using 131 colonies had more characters with which to distinguish the species than the analysis using 51 colonies. Finally, the analysis using 131 colonies had more colonies than the analysis using 51 colonies, which made it easier to discriminate between species due to more robust sample sizes. Despite these differences, the similarity between the two analyses of correctly assigning most colonies (95% and 98%) indicates the quantitative data support the qualitative species groupings.

TABLE 2—Amount of variation explained by each discriminant function from the analysis using 131 colonies and 14 quantitative characters. * Indicates function did not significantly contribute to discrimination at $P = 0.05$.

| Function | % of variation | Cumulative % |
|---|---|---|
| 1 | 94.03 | 94.03 |
| 2 | 3.00 | 97.03 |
| 3 | 1.77 | 98.80 |
| 4 | 0.90 | 99.70 |
| 5 | 0.17 | 99.87 |
| 6 | 0.09 | 99.96 |
| 7* | 0.04 | 100.00 |

TABLE 3—Character loadings on the discriminant functions from the analysis using 131 colonies and 14 quantitative characters. Character numbers refer to Appendix 1.

| Character # | Function 1 | 2 | 3 | 4 | 5 | 6 |
|---|---|---|---|---|---|---|
| 55 | 0.900 | −0.129 | 0.136 | −0.074 | 0.084 | −0.310 |
| 44 | 0.146 | 0.529 | 0.362 | 0.321 | −0.057 | −0.420 |
| 49 | −0.040 | −0.266 | 0.716 | −0.333 | 0.054 | −0.248 |
| 54 | −0.047 | −0.329 | −0.570 | 0.216 | 0.162 | −0.374 |
| 43 | 0.034 | 0.263 | 0.459 | −0.231 | 0.289 | 0.047 |
| 52 | −0.044 | −0.229 | 0.302 | 0.246 | 0.166 | 0.005 |
| 41 | 0.029 | 0.245 | 0.250 | −0.064 | 0.095 | −0.038 |
| 42 | 0.003 | 0.515 | 0.095 | 0.609 | −0.312 | −0.429 |
| 51 | −0.023 | −0.373 | 0.270 | 0.557 | 0.367 | 0.291 |
| 45 | 0.132 | 0.106 | −0.334 | 0.528 | −0.410 | −0.121 |
| 50 | −0.008 | −0.184 | 0.087 | 0.230 | 0.042 | 0.126 |
| 46 | 0.001 | 0.645 | −0.299 | 0.011 | 0.673 | −0.068 |
| 53 | −0.059 | −0.201 | 0.105 | 0.149 | 0.483 | −0.111 |
| 48 | 0.018 | 0.109 | 0.022 | −0.119 | 0.202 | −0.178 |

## PHYLOGENY RECONSTRUCTION

To understand the phylogenetic relationships among the eight species, cladistic methodology was used. The 40 multistate morphologic characters (characters 1–40 in Appendix 1) were used in the cladistic analysis. The states of each character for the eight ingroup species and two outgroup species are listed in Appendix 2. Cladistic analysis was performed with PAUP (Swofford, 1985), the parsimony-based cladistic software package. The "branch and bound" algorithm was used because it is most successful at finding the most parsimonious cladogram (Hendy and Penny, 1982; Swofford, 1985).

No a priori assumptions regarding the transformational ordering of character states were made before analysis. By using unordered characters, any character state could potentially evolve directly into any other state. The ordering of states (i.e., placing them in a polarity sequence from plesiomorphic to apomorphic) was done simultaneously with the cladistic analysis using outgroup analysis. Outgroup species were restricted to those taxa that do not exhibit morphology similar to the ingroup. Species of the families Halloporidae and Amplexoporidae were excluded because they probably evolved from species of the family Bimuroporidae. Halloporids and bimuroporids both have closely spaced diaphragms in early zooecial ontogeny. Evolution of the halloporids from the bimuroporids is currently being analyzed by the author and evolution of the amplexoporids from the bimuroporids has been argued by Ross (1964). Ross proposed that a Middle Ordovician species of *Champlainopora* gave rise to *Amplexopora*. This hypothesis is supported by their shared characters of remnant growing tips in endozone, integrate wall structure, few mesozooids, polygonal autozooecial cross sections in the endozone and exozone, and presence of acanthostyles (at least in the more derived species of *Champlainopora*). The hypothesis that *Amplexopora* evolved from *Champlainopora* is also supported by their relative stratigraphic positions. *Champlainopora* originated in the lower Chazyan and became extinct in the lower Kirkfieldian. *Amplexopora* originated in the lower Kirkfieldian and continued well into the Upper Ordovician.

Two species of *Eridotrypa* were chosen for the outgroup because they are definitely not members of the ingroup, but they have been closely associated with members of the ingroup in previous classifications. Astrova (1978) noted the similarity of *Eridotrypa* and *Champlainopora* and made *Champlainopora* a junior synonym of *Eridotrypa*. Pushkin also noted the relatedness of *Champlainopora* and *Eridotrypa* by placing them in the same family, Trematoporidae (Ropot and Pushkin, 1987).

These two genera are similar in that their type species have small pustules at the autozooecial wall boundaries in the exozone (compare Figure 9.8 with Ross, 1967, Pl. 71, fig. 6). These two genera share the same integrate wall structure, the same ordered zooidal arrangement, and they both have large, long, axial zooids that bud off smaller, shorter zooids. They differ in their budding patterns; *Eridotrypa* exhibits an intrazooidal pattern, whereas *Champlainopora* exhibits an interzooidal pattern (McKinney, 1977). This morphologic comparison suggests that *Champlainopora* and *Eridotrypa* are sister taxa that evolved from a common ancestor. Other than the eridotrypids, there are few other possible sister groups because this fauna occurs so early in the evolutionary development of the trepostomes.

Using only one outgroup species can produce misleading character polarities due to autapomorphic characters in the outgroup species. To reduce this problem, two species of *Eridotrypa* were chosen. One was the type species: *Eridotrypa mutabilis* Ulrich, 1893. The other was the oldest species of *Eridotrypa* found in the Simpson Group (referred to in the figures and tables as *Eridotrypa* sp.). It occurs in the lower part of the Oil Creek Formation (Farmer, 1974). The character states for both species are listed in Appendix 2.

## CLADISTIC RESULTS

Using all 40 multistate characters, cladistic analysis resulted in 19 equally parsimonious cladograms. Each of the 19 cladograms had a length of 41 steps and a consistency index of 0.756. Instead of discussing all 19 cladograms separately, a strict consensus cladogram was produced. This was done with the computer software package CONTREE (Swofford, 1986). The resulting consensus cladogram is shown in Figure 5. It shows that all members of the ingroup (family Bimuroporidae) share a common ancestor. Within the ingroup, two groups of species are evident. First near the base, the three least derived species of the ingroup (*Champlainopora chazyensis, C. ramusculus,* and *C. pachymura*) form a polychotomy. The first group is separated from the second group by *C. arbucklensis*. The second group also forms a polychotomy containing the most derived ingroup species (*Bimuropora dubia, B. pollaphragmata, B. conferta,* and *B. winchelli*).

The placement of *C. arbucklensis* with the other species of *Champlainopora* was based on the distribution of growth-pattern characters. This was done using a cladogram constructed from the six characters concerned with growth pattern (characters 5–10 in Appendix 1). These growth-pattern characters are less likely to be convergent because they are the first occurrences so far known of these growth patterns in the fossil record. They are probably true apomorphies because there are neither potential ancestors nor time to make a plausible argument for convergence. The probable homologous nature of the growth-pattern character states is partially supported by the other 34 characters unassociated with growth pattern.

A cladistic analysis was performed using only the six growth-pattern characters. The resulting consensus cladogram is shown in Figure 6. The growth-pattern characters reveal a cladogram (Figure 6) similar to that produced by all 40 characters (Figure 5). The main difference is the position of *Champlainopora arbucklensis*. In Figure 5 it was not immediately grouped with any other species while in Figure 6 it was grouped with the other species of *Champlainopora*. Other than this one difference, both cladograms are identical. Figure 6 served as the basis for grouping the species into genera.

This classification is supported by the results from a different cladistic analysis. Instead of using outgroup analysis to determine character polarities, the stratigraphically oldest species (*Champlainopora chazyensis*) was used. In this analysis, *C. chazyensis* served as the ancestor for determining the primitive character states. Both analyses produced the same classification.

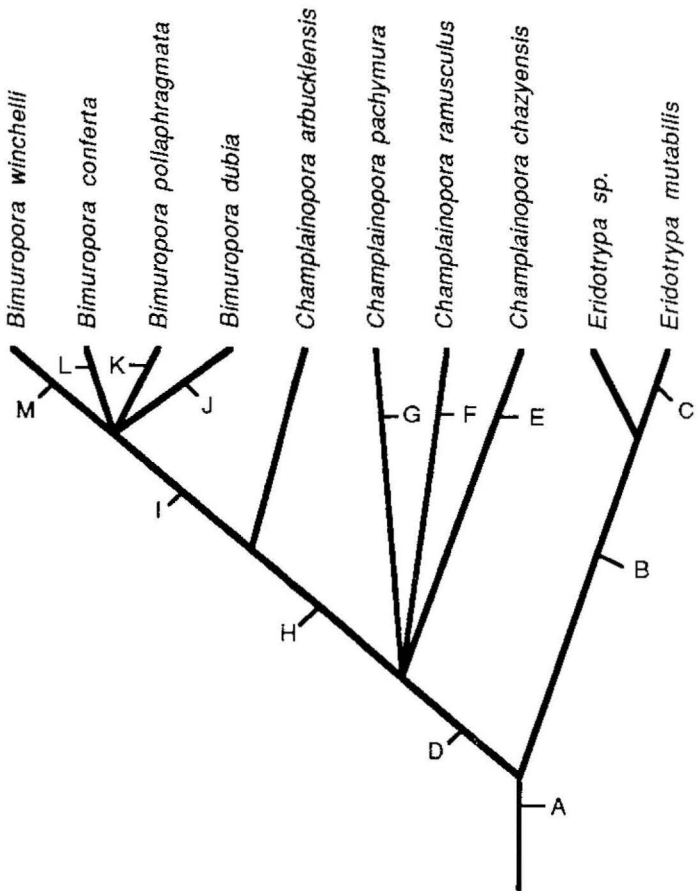


FIGURE 5—Consensus cladogram using all 40 multistate characters. Letters refer to synapomorphic character states listed in Appendix 3.

## SYSTEMATIC PALEONTOLOGY

Phylum BRYOZOA Ehrenberg, 1831
Class STENOLAEMATA Borg, 1926
Order TREPOSTOMATA Ulrich, 1882
Family BIMUROPORIDAE n. fam.

*Type genus.*—*Bimuropora* n. gen.

*Diagnosis.*—Trepostome with ramose growth habit; remnant growing tips in endozone; interzooecial budding pattern; zooecia commonly begin ontogeny as mesozooecia and expand into autozooecia; autozooecial wall structure integrate with wall laminae sharply convex distally; mesozooecia rare and in exozone occur in corners of adjacent autozooecia; diaphragms and acanthostyles common.

*Description.*—Zoaria ramose. Branch cross-sectional shape circular. Maculae commonly but not always present. Remnant growing tips as evinced by zooecial wall thickening in endozone present. Budding pattern interzooecial. Zooecial arrangement ordered or disordered; most zooecia characterized by ontogenetic progression of mesozooecia expanding into autozooecia; zooecia gradually expand distally through early ontogeny, curve outward toward colony surface. Mesozooecial stage of early zooecial ontogeny abbreviated. After mesozooecial stage, diaphragms widely spaced in endozone, closely spaced in exo-

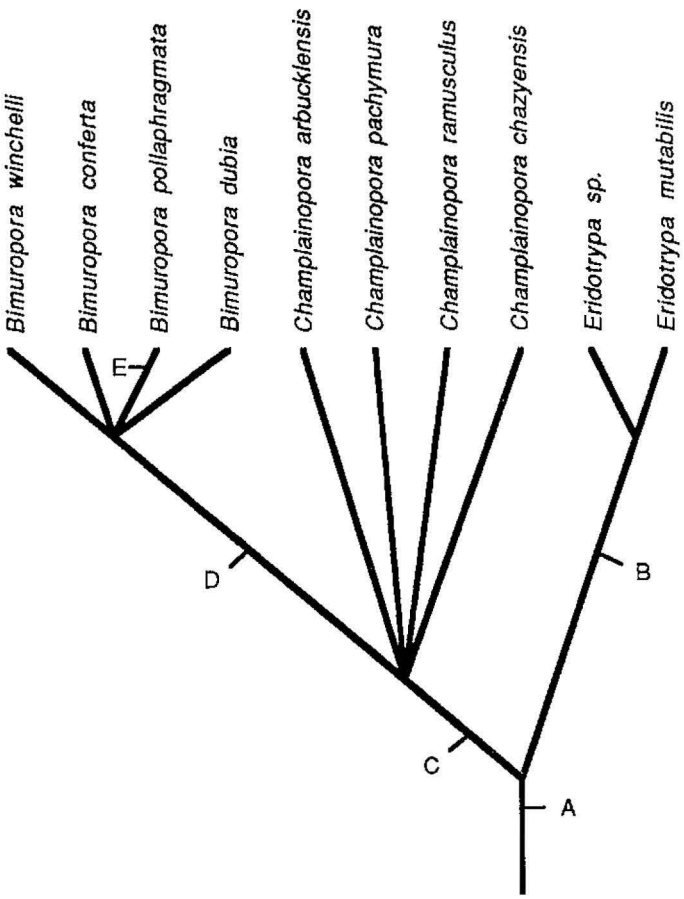


FIGURE 6—Consensus cladogram using only the multistate characters associated with growth pattern. Letters refer to synapomorphic character states listed in Appendix 4.

zone. Zooecial walls in endozone regular, crenulated, or wavy where autozooecia adjacent, generally regular where autozooecia and mesozooecia adjacent. Autozooecial wall structure in exozone integrate, boundary irregular or straight; wall laminae sharply convex distally; autozooecial living chamber cross-sectional shape changes ontogenetically from polygonal in endozone to subpolygonal in exozone; autozooecial basal diaphragms planar or cystoidal. Cystiphragms absent. Mesozooecia rare, only occur in corners of adjacent autozooecia; mesozooecial walls thinner than those of autozooecia. Acanthostyles abundant when present. Mural spines and cap-like apparati (sensu Conti and Serpagli, 1987) absent.

*Discussion.*—The growth pattern exhibited by bimuroporids is similar to, but not the same as, that in family Halloporidae. In halloporids the ontogenetic transformation of mesozooecia into autozooecia is consistently developed in all zooecia. In the bimuroporids it is not. When it is developed in the bimuroporids it superficially resembles that of the halloporids, but upon closer analysis the two are distinctly different. The early zooecial ontogeny of halloporids is generally characterized by a more extended mesozooecial stage, more closely spaced diaphragms in this stage, and a more gradual zooecial expansion. The early zooecial ontogeny of the bimuroporids is generally characterized by a shorter mesozooecial stage, generally less closely spaced diaphragms in this stage, and a less gradual zooecial expansion.

Remnant growing tips in the endozone are rare or absent in the family Halloporidae, while in the family Bimuroporidae they are present. Remnant growing tips are poorly developed in bimuroporids relative to some trepostomes (e.g., Boardman, 1960). This probably reflects extensive resorption of the thick exozonal walls that formed on the growing tip. This may indicate that the bimuroporids followed a model of morphogenesis as proposed by Boardman (1960).

The autozooecial living chamber cross-sectional shape changes ontogenetically. A zooecium begins with a polygonal shape, and as it expands it becomes subpolygonal. This results from the zooecial walls coming into contact with increasingly more adjacent zooecia. The lack of abundant space-filling mesozooecia in the endozone prohibits the existence of circular autozooecia like the halloporids. This pattern is evinced in transverse section where newly budded autozooecia have a small polygonal cross section, while large older autozooecia have a large subpolygonal cross section.

Autozooecial wall structure is generally amalgamate in halloporids (except for older species). In bimuroporids it is integrate. Cystoidal basal diaphragms are rare if at all present in halloporids, but very common in bimuroporids. Unlike halloporids, bimuroporids usually have acanthostyles.

Family Bimuroporidae contains characteristics of both family Halloporidae and Amplexoporidae. Members of family Bimuroporidae have a growth pattern like that of halloporids, but have very few mesozooecia and a wall structure like amplexoporids. Family Bimuroporidae includes species previously assigned to both the Halloporidae and Amplexoporidae. Ross (1964) proposed that *Amplexopora* (the type genus of family Amplexoporidae) evolved from *Champlainopora* (a genus in family Bimuroporidae). Ross based this hypothesis on their similar integrate wall structure and paucity of mesozooids. The more derived species of *Champlainopora* even have acanthostyles like *Amplexopora.* The founding species of *Amplexopora* may have evolved from some species of *Champlainopora* by 1) a reduction in the number of mesozooids and 2) a loss of diaphragms in early zooidal ontogeny. Amplexoporids lack the intrazooidal transformation of mesozooids to autozooids.

This close phylogenetic association between halloporids and amplexoporids is in direct conflict with the classification proposed by Astrova (1965, 1978). Astrova's subdivision of the order Trepostomata is based on the distribution of polymorphs. Astrova's suborder Halloporoidea is characterized by few acanthostyles and many mesozooecia while suborder Amplexoporoidea is characterized by exilazooecia, many small acanthostyles, and few mesozooecia. The results of this report support the use of not only the types of polymorphs, but also wall structure and growth-pattern characters in organizing higher taxa.

Based on the above description, the following genera are included in this concept of family Bimuroporidae: *Bimuropora* n. gen. and *Champlainopora* (Ross, 1970).

*Occurrence.*—Members of family Bimuroporidae have been reported in North America and Europe. They occur only in the Middle Ordovician.

### Genus BIMUROPORA n. gen.

*Etymology.*—The name is derived from *bi,* the Latin adjective for two, and *murus,* the Latin noun for wall. This is in reference to the integrate wall structure.

*Type species.*—*Hallopora dubia* Loeblich, 1942, p. 430, Pl. 62, figs. 8–11.

*Diagnosis.*—Bimuroporid with maculae composed of megazooecia and mesozooecia; disordered zooecial arrangement; wide endozone; large axial ratio; irregular wall boundaries.

*Description.*—Maculae present, composed of cluster of mega-

zooecia and mesozooecia. Zooecial arrangement disordered; zooecia all have same general length as a result of disordered zooecial arrangement. Zooecial cross-sectional shape changing in conjunction with ontogenetic progression from polygonal to subpolygonal, growth pattern evident in transverse section as an even distribution of small polygonal and large subpolygonal zooecia throughout endozone; endozones wide, axial ratios large. Autozooecial wall boundary in exozone irregular; autozooecial walls in exozone thin; autozooecial basal diaphragm shape planar, concave, convex, or cystoidal; spacing variable. Zooecial walls in endozone generally straight, occasionally crenulated where autozooecia adjacent, occasionally fluted where autozooecia and mesozooecia adjacent. Acanthostyles present.

*Discussion.*—Based on the above description, the following species are herein assigned to this concept of *Bimuropora*: *Amplexopora winchelli* Ulrich, 1886; *Batostoma conferta* Coryell, 1921; *Batostoma decipiens* Ulrich, 1893; *Batostoma dendroidea* Coryell, 1921; *Bimuropora pollaphragmata* n. gen. and sp.; *Hallopora dubia* Loeblich, 1942.

*Champlainopora* (Ross, 1970) differs from *Bimuropora* in having an ordered zooecial arrangement with long, large, axial zooecia, narrower endozones, smaller axial ratios, generally smaller autozooecial apertural areas, and thicker autozooecial walls in the exozone. *Champlainopora* (Ross, 1970) is also stratigraphically older than *Bimuropora*.

*Occurrence.*—Species here assigned to *Bimuropora* have been reported in Oklahoma (Loeblich, 1942), Alabama (McKinney, 1971), Tennessee (Coryell, 1921), Kentucky (Brown, 1965), Illinois, Wisconsin, and Iowa (Perry, 1962; Bork and Perry, 1967), Minnesota (Ulrich, 1886 and 1893), New York (Ross, 1969), and possibly from Estonia (Bassler, 1911) and Canada (Fritz, 1957). These occurrences place the range of the genus in the Blackriveran, Rocklandian, and Kirkfieldian Stages of the Middle Ordovician.

BIMUROPORA DUBIA (Loeblich, 1942)
Figure 7.1–7.5

*Hallopora dubia* LOEBLICH, 1942, p. 430, Pl. 62, figs. 8–11.
?*Hallopora dubia* (Loeblich). ASTROVA, 1965, p. 174–175, text fig. 32, Pl. 22, fig. 1; MERIDA AND BOARDMAN, 1967, Pl. 100, fig. 3; KANYGIN, OBUT, VOLKOVA, AND YAROSHINSKAYA, 1984, p. 25, Pl. 17, fig. 3.

*Description.*—Irregularly shaped, elevated maculae present. All zooecia develop mesozooecial stage in early ontogeny. Mean surface angle 75.4°; mean endozone diameter 3.53 mm; mean exozone width 0.64 mm; mean zoarial branch diameter 4.80 mm; mean axial ratio 0.73; mean autozooecial living chamber cross-sectional area in exozone 0.035 mm$^2$; mean autozooecial living chamber depth 0.333 mm; assuming cylindrical shape for autozooecial living chambers, mean volume 0.012 mm$^3$; mean autozooecial wall thickness in exozone 0.050 mm. Autozooecial basal diaphragms intersect walls at varying angles; shape planar, convex, or cystoidal, occasionally concave; mean spacing 0–13 per mm. Mean number of diaphragms per mm in mesozooecial stage of early ontogeny 8.7, decreasing to 1.1 in remaining endozone, increasing in exozone to 7.5. Walls of adjacent autozooecia in endozone straight or crenulated; walls of mesozooecia in endozone fluted. Acanthostyles present (mean = 13.4/mm$^2$), small, occur only in corners of adjacent autozooecia. (All qualitative character states are listed in Appendix 1 and quantitative data are summarized in Appendix 5.)

*Discussion.*—When describing *Hallopora dubia,* Loeblich (1942, p. 430) noted that the acanthostyles and wall structure were "features which are not characteristic of *Hallopora.*" Loeblich's doubt in assigning this species to *Hallopora* is also evident in his choice of its species name: *dubia.*

*Bimuropora dubia* differs from all other species of *Bimuropora* in having a more consistently developed mesozooecial stage in early zooecial ontogeny, more abundant diaphragms in this stage, and slightly constricted walls where diaphragms insert in early ontogeny. *Bimuropora dubia* is similar to *B. dendroidea* (Coryell, 1921) except that *B. dendroidea* (Coryell, 1921) has more abundant acanthostyles, larger autozooecial living chambers, and more abundant mesozooecia. A discriminant analysis like the one described earlier was run with the addition of Coryell's (1921) holotype of *Batostoma dendroidea* (USNM 44731). In the classification phase of this analysis, the colonies of *Bimuropora dubia* were never grouped with the holotype of *Bimuropora dendroidea.*

→

FIGURE *7—1–5, Bimuropora dubia* (Loeblich). *1,* remnant growing tip in endozone, USNM 435401, USNM locality 2132X$_9$, longitudinal section, ×50; *2,* autozooecial wall thickening in exozone, crenulated integrate wall boundary, acanthostyle in upper wall, USNM 435401, USNM locality 2132X$_9$, longitudinal section, ×100; *3,* small, younger zooecia with polygonal cross-sectional shapes and large, older zooecia with subpolygonal cross-sectional shapes, USNM 435400, USNM locality 2132X$_9$, slightly oblique transverse section, ×30; *4,* growth pattern with closely spaced diaphragms in early zooecial ontogeny followed by widely spaced diaphragms in later ontogeny, slightly constricted (fluted) walls at diaphragm attachment, locally crenulated zooecial walls in endozone, USNM 435398, USNM locality 2132X$_7$, longitudinal section, ×30; *5,* subpolygonal autozooecial apertures, integrate wall structure, small acanthostyles at zooecial corners, macular megazooecia and mesozooecia in upper center, USNM 100497, USNM locality 2189, tangential section, ×30. *6, 7, Bimuropora pollaphragmata* n. gen. and sp. *6,* zooecial wall thickening in exozone, crenulated integrate wall boundaries, varied autozooecial basal diaphragm shapes, acanthostyles at bottom, USNM 435406, USNM locality 2127J, longitudinal section, ×100; *7,* growth pattern with closely spaced diaphragms in early zooecial ontogeny and abundant diaphragms throughout rest of ontogeny, USNM 435406, USNM locality 2127J, longitudinal section, ×30.

FIGURE *8—1–3, Bimuropora pollaphragmata* n. gen. and sp. *1,* small, younger zooecia with polygonal cross-sectional shapes and large, older zooecia with subpolygonal cross-sectional shapes, USNM 435419, USNM locality 2127J, slightly oblique transverse section, ×30; *2,* remnant growing tip in endozone, USNM 435407, USNM locality 2127J, longitudinal section, ×50; *3,* abundant acanthostyles surrounding zooecia, subpolygonal autozooecial aperture shape in exozone, integrate wall structure, USNM 435408, USNM locality 2127J, tangential section, ×50. *4–9, Bimuropora conferta* (Coryell); *4,* thin zooecial walls in exozone with integrate wall structure, subpolygonal autozooecial apertures often inflected by large acanthostyles, USNM 435428, USNM Locality 2132X$_1$, tangential section, ×50; *5,* growth pattern with few closely spaced diaphragms in early zooecial ontogeny followed by widely spaced diaphragms in later ontogeny, elevated macula with megazooecium and mesozooecium in upper right, USNM 435429, USNM locality 2132X$_1$, longitudinal section, ×30; *6,* small, younger zooecia with polygonal cross-sectional shapes and large, older zooecia with subpolygonal cross-sectional shapes, USNM 435421, USNM locality 2132X$_1$, transverse section, ×30; *7,* remnant growing tip in endozone, USNM 435423, USNM locality 2132X$_1$, longitudinal section, ×50; *8,* closely spaced autozooecial basal diaphragms in thick exozone, USNM 435424, USNM locality 2132X$_1$, longitudinal section, ×30; *9,* crenulated integrate wall boundary, acanthostyle in upper wall, distally concave and planar autozooecial basal diaphragms, USNM 435424, USNM locality 2132X$_1$, longitudinal section, ×100.

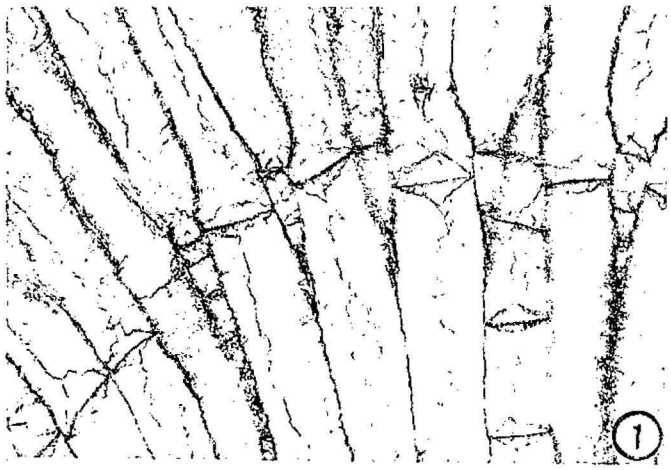
1


2

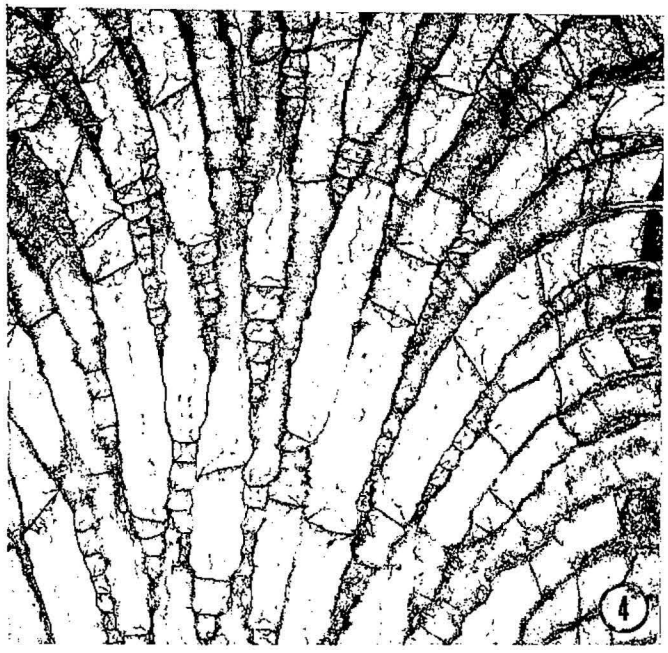
4

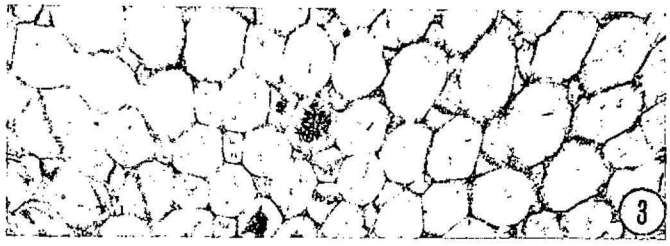
3

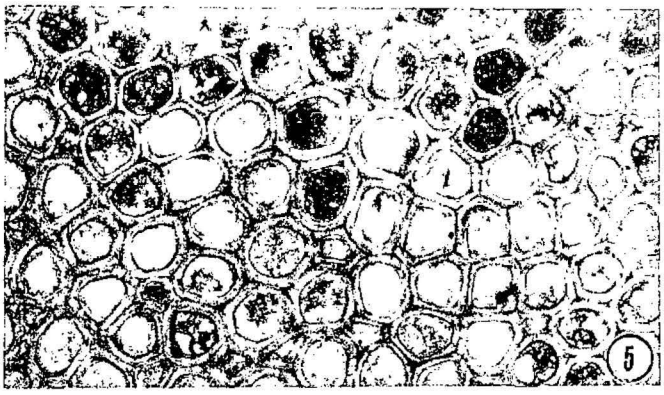
5

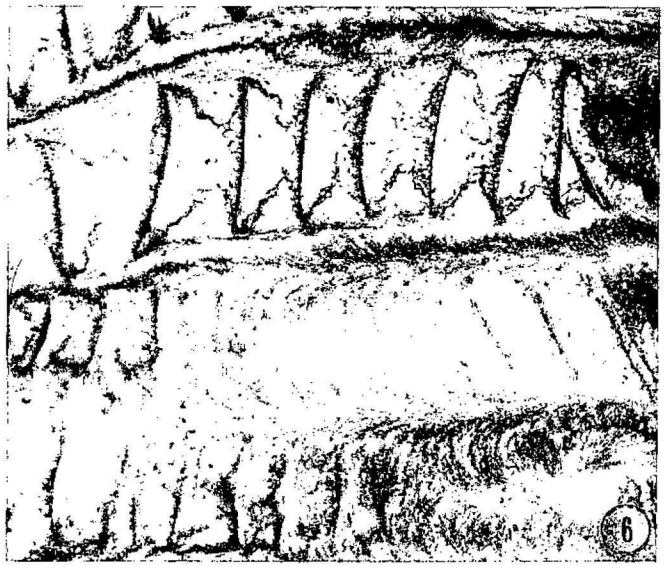
6

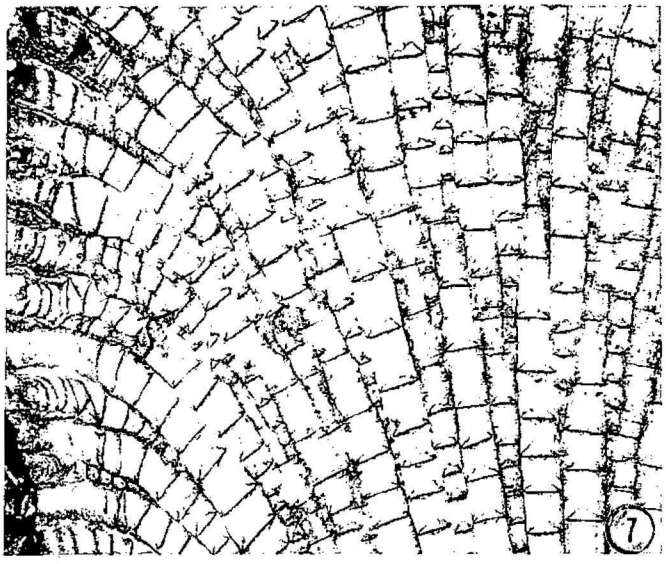
7

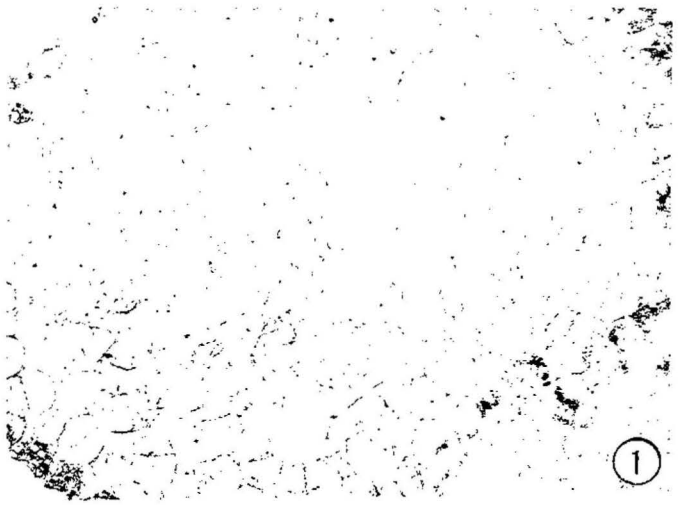
1


2

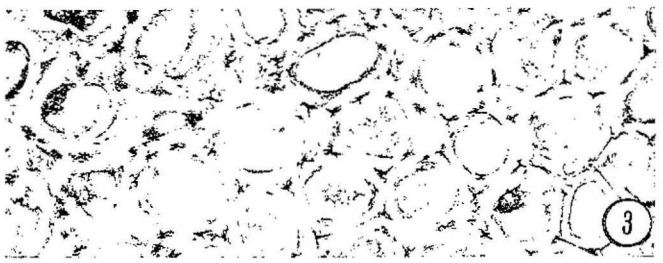
3

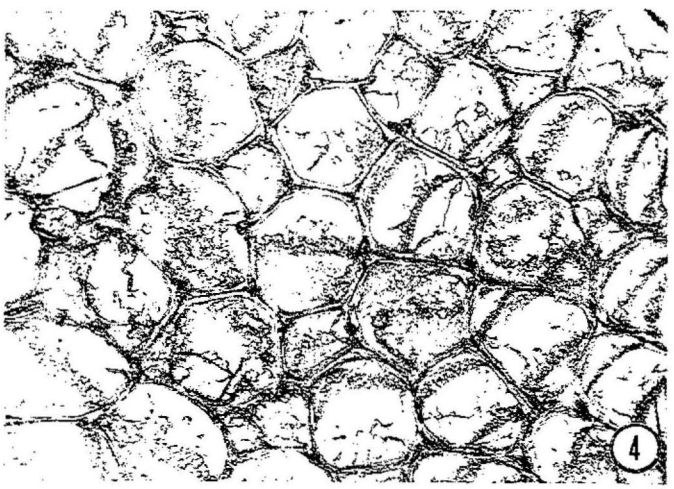
4

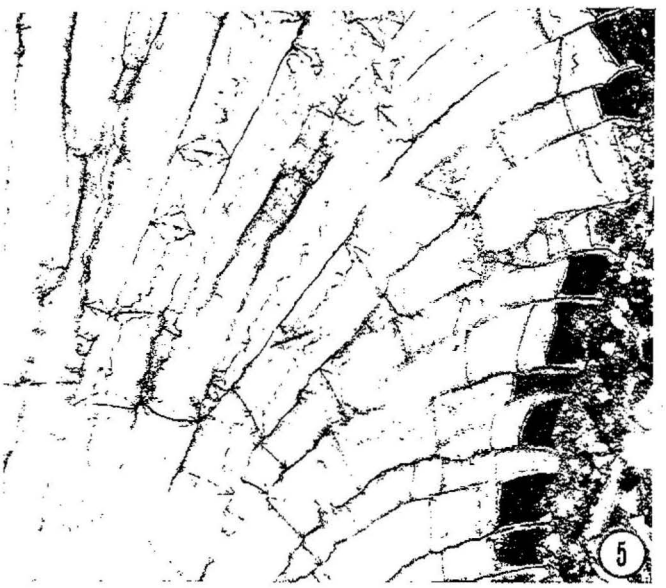
5

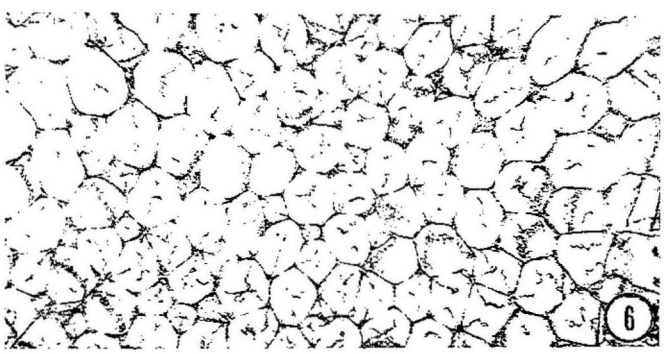
6

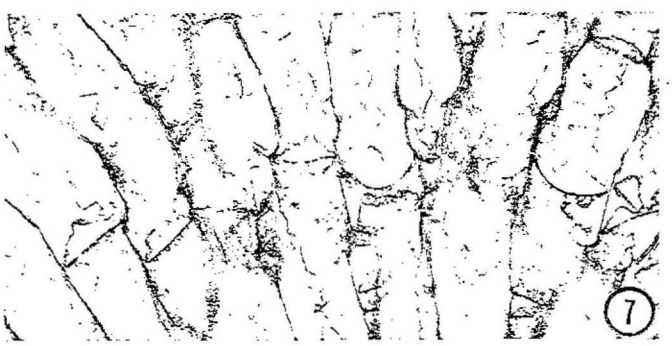
7

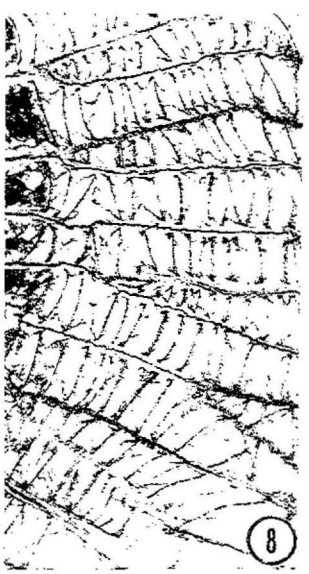
8


9

*Material.*—The following material was measured and/or figured: holotype USNM 100497 (Loeblich's holotype of *Hallopora dubia*); hypotypes USNM 435394–435405.

*Occurrence.*—*Bimuropora dubia* has been reported in the Bromide Formation in Oklahoma (Loeblich, 1942). Specimens were found immediately below the Corbin Ranch Submember in the Pooleville Member of the Bromide Formation. These occurrences place the range of the species in the Blackriveran Stage (Ross et al., 1982). Oklahoma specimens came from USNM localities 2132$X_5$, $X_7$, $X_9$, and 2189. Loeblich's type material of *Hallopora dubia* came from locality 2189, which is geographically and stratigraphically equivalent to the 2132X localities.

### BIMUROPORA POLLAPHRAGMATA n. sp.
Figures 7.6, 7.7, 8.1–8.3

*Etymology.*—The name is derived from *polla,* the plural form of the Greek adjective for many, and *phragmata,* the plural form of the Greek noun for partition. This is in reference to the abundant autozooecial diaphragms.

*Diagnosis.*—*Bimuropora* with low surface angle; thin exozone; small autozooecial living chamber cross-sectional area in exozone; closely spaced basal zooecial diaphragms throughout ontogeny.

*Description.*—Irregularly shaped, elevated maculae present. All zooecia develop mesozooecial stage in early ontogeny. Surface angle low (mean = 66.7°). Mean endozone diameter 2.82 mm; exozones thin (mean = 0.46 mm); mean zoarial branch diameter 3.74 mm; mean axial ratio 0.75. Autozooecial living chambers in exozone small (mean cross-sectional area = 0.023 mm$^2$, mean living chamber depth = 0.278 mm); assuming cylindrical shape for autozooecial living chamber, mean volume 0.006 mm$^3$; mean autozooecial wall thickness in exozone 0.050 mm. Autozooecial basal diaphragms intersect walls at varying angles; shape planar, convex, or cystoidal, occasionally concave; mean spacing 4–18 per mm. Autozooecial basal diaphragms generally closely spaced throughout ontogeny; mean number of diaphragms 10.0/mm in mesozooecial stage of early ontogeny, decreasing to 4.4 in remaining endozone, increasing in exozone to 10.4. Autozooecial and mesozooecial walls in endozone generally straight. Acanthostyles very abundant (mean = 24.4/mm$^2$), small, surround autozooecia but do not inflect zooecial walls. (All qualitative character states are listed in Appendix 1 and quantitative data are summarized in Appendix 6.)

*Discussion.*—Unlike all other species of *Bimuropora, B. pollaphragmata* has closely spaced diaphragms throughout zooecial ontogeny. The other species only have closely spaced diaphragms in early and late ontogeny. Relative to other species in the genus, *B. pollaphragmata* has the smallest autozooecial living chamber apertural areas, thinnest exozones, smallest surface angles, and shallowest autozooecial living chambers.

*Material.*—The following material was measured and/or figured: holotype USNM 435406; paratypes USNM 435407–435419.

*Occurrence.*—Specimens of *Bimuropora pollaphragmata* were found in the upper part of the Mountain Lake Member of the Bromide Formation. This places the range of the species in the middle part of the Blackriveran Stage (Ross et al., 1982). Specimens came from USNM locality 2127J.

### BIMUROPORA CONFERTA (Coryell, 1921)
Figure 8.4–8.9

*Batostoma conferta* CORYELL, 1921, p. 295, Pl. 10, figs. 1–3.
*Amplexopora conferta* (Coryell). ROSS, 1969, p. 265, Pl. 35, figs. 1–4.

*Description.*—Irregularly shaped, elevated maculae present. Not all zooecia develop mesozooecial stage in early ontogeny. Surface angles high (mean = 79.1°). Mean endozone diameter 3.00 mm; mean exozone width 0.83 mm; mean zoarial branch diameter 4.67 mm; mean axial ratio 0.66; mean autozooecial living chamber cross-sectional area in exozone 0.052 mm$^2$; mean living chamber depth 0.318 mm; assuming cylindrical shape for autozooecial living chambers, mean volume 0.017 mm$^3$; autozooecial walls in exozone thin (mean = 0.044 mm). Autozooecial basal diaphragms intersect walls at varying angles; shape usually planar, convex, or cystoidal, occasionally concave; mean spacing 0–13 per mm. Mean number of diaphragms 7.2/mm in mesozooecial stage of early ontogeny, decreasing to 0.5 in remaining endozone, increasing in exozone to 6.4. Autozooecial and mesozooecial walls in endozone generally straight. Acanthostyles abundant (mean = 19.5/mm), commonly large, surround autozooecia, inflect walls. (All qualitative character states are listed in Appendix 1 and quantitative data are summarized in Appendix 7.)

*Discussion.*—The size and abundance of acanthostyles are highly variable. Coryell (1921) also noted the irregular distribution of large acanthostyles. In the Simpson Group material, large acanthostyles are absent in some parts of a colony and are completely lacking in some colonies.

*Bimuropora conferta* differs from most other species of *Bimuropora* in having a poorly developed mesozooecial stage in early ontogeny, widely spaced diaphragms in the endozone, and large acanthostyles that commonly inflect the autozooecial walls. *Bimuropora winchelli* (Ulrich, 1886) differs from *B. conferta* in having smaller acanthostyles that do not inflect the zooecial walls.

*Material.*—The following material was measured and/or figured: holotype USNM 44736 (Coryell's holotype of *Batostoma conferta*); hypotypes USNM 435420–435431.

*Occurrence.*—*Bimuropora conferta* has been reported in the Pierce Limestone in central Tennessee (Coryell, 1921) and the Chaumont Formation in northeast New York (Ross, 1969). In

→

FIGURE 9—*1–5, Bimuropora winchelli* (Ulrich). *1,* thin zooecial walls in exozone, subpolygonal autozooecial apertures, small acanthostyles at zooecial corners, integrate wall structure, USNM 435445, USNM locality 2132$X_{15}$, tangential section, ×30; *2,* small, younger zooecia with polygonal cross-sectional shapes and large, older zooecia with subpolygonal cross-sectional shapes, USNM 435445, USNM locality 2132$X_{15}$, transverse section, ×30; *3,* remnant growing tip and locally crenulated zooecial walls in endozone, USNM 435443, USNM locality 2132$X_{15}$, longitudinal section, ×50; *4,* zooecial wall thickening in exozone, crenulated integrate wall boundaries, distally convex autozooecial basal diaphragms, USNM 435446, USNM locality 2132$X_{15}$, longitudinal section, ×100; *5,* growth pattern with closely spaced diaphragms in early zooecial ontogeny followed by widely spaced diaphragms in later ontogeny, high surface angle, USNM 435446, USNM locality 2132$X_{15}$, longitudinal section, ×30. *6–9, Champlainopora chazyensis* (Ross). *6,* growth pattern with closely spaced diaphragms in early zooecial ontogeny and widely spaced diaphragms in later ontogeny, intermediate surface angle, USNM 435450, USNM locality 2114E, longitudinal section, ×30; *7,* thick zooecial walls with mesozooecial apertures completely filled in and autozooecial apertures partially filled in, integrate wall structure, USNM 435450, USNM locality 2114E, tangential section, ×30; *8,* subpolygonal autozooecial apertures in exozone, integrate wall structure, pustules along zooecial boundaries, USNM 435454, USNM locality 2115B, tangential section, ×50; *9,* large, older subpolygonal axial zooecia surrounded by small, younger polygonal zooecia, USNM 435455, USNM locality 2129N, transverse section, ×30.

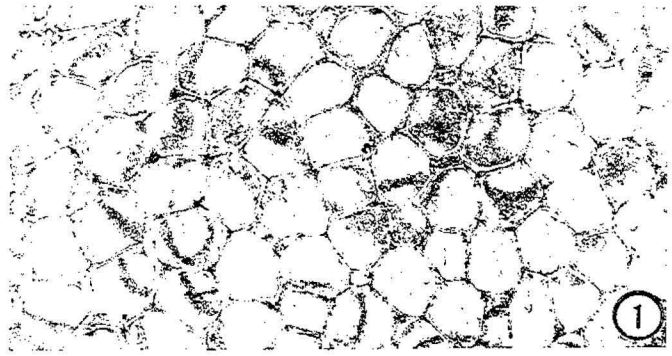
1

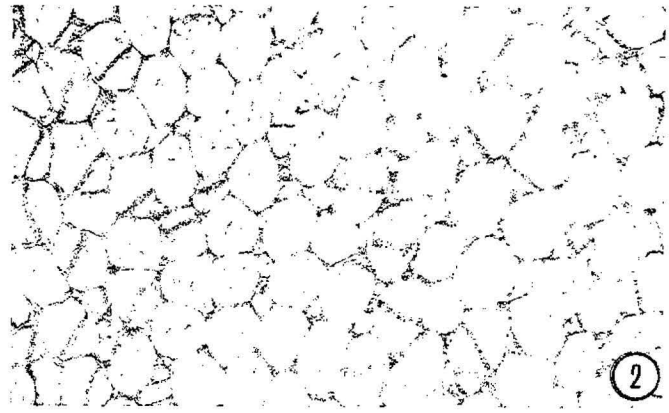
2


3


4

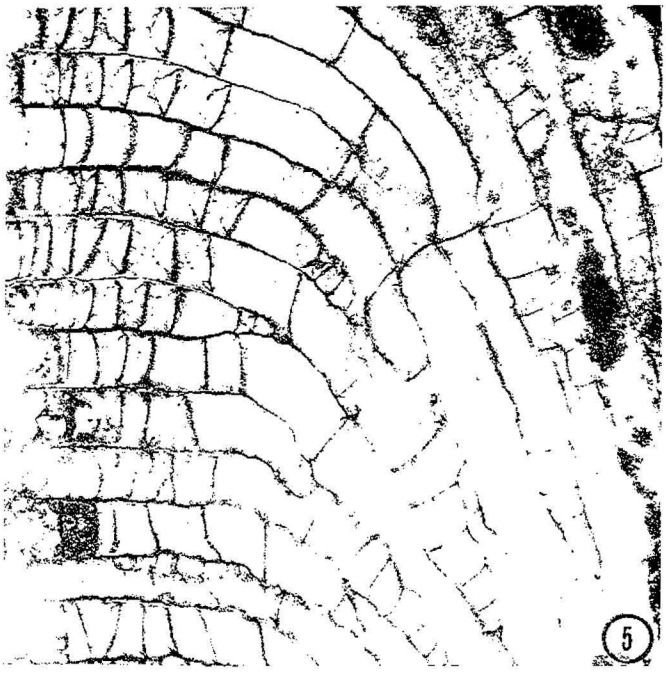
5

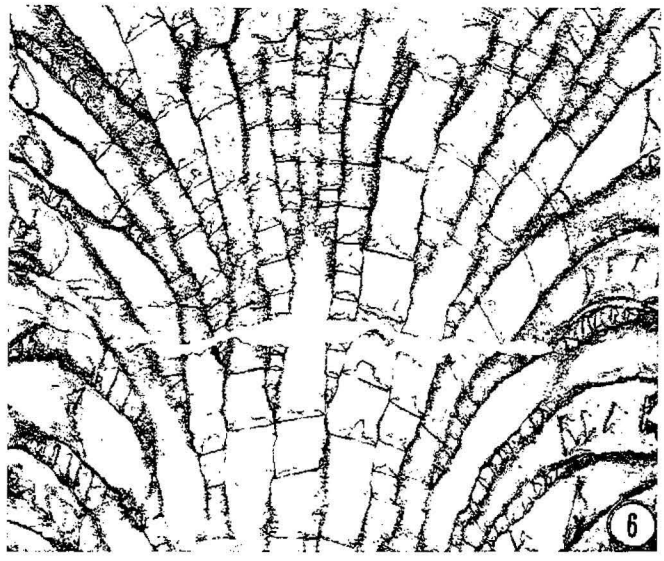
6

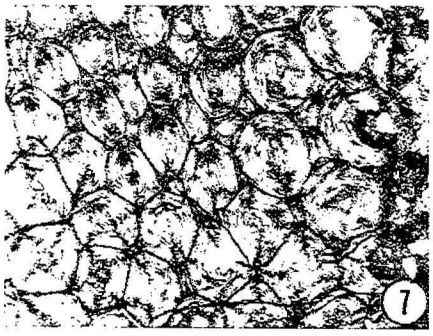
7

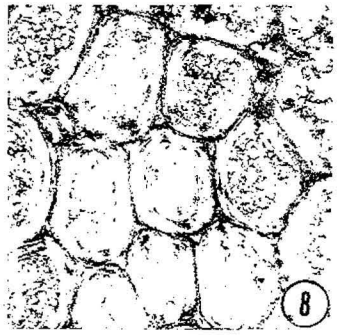
8

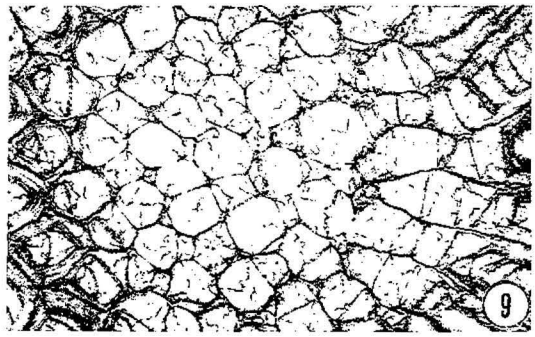
9

Oklahoma, specimens were found immediately below the Corbin Ranch Submember in the Pooleville Member of the Bromide Formation. These occurrences place the range of the species in the Blackriveran Stage (Ross et al., 1982). Oklahoma specimens came from USNM localities 2132X$_1$ and X$_3$.

### BIMUROPORA WINCHELLI (Ulrich, 1886)
Figure 9.1–9.5

*Amplexopora winchelli* ULRICH, 1886, p. 91–92; MCKINNEY, 1971, p. 250–255, Pl. 54, figs. 1–8, Pl. 55, figs. 1–3; BROWN, 1965, p. 1002–1003, Pl. 118, figs. 8–10; BORK AND PERRY, 1967, p. 1374–1375, Pl. 173, figs. 1, 2, 7–9; ROSS, 1969, p. 265, Pl. 37, figs. 2–4.

*Batostoma winchelli* (Ulrich). ULRICH, 1893, p. 295–296, Pl. 26, figs. 33, 34, 36, 37, Pl. 27, figs. 1–6; WILSON, 1921, Pl. 2, figs. 7, 8; LOEBLICH, 1942, p. 432–433, Pl. 64, figs. 8–10; PERRY, 1962, p. 26–28, Pl. 6, figs. 4–11.

*Batostoma chapparsi* LOEBLICH, 1942, p. 431, Pl. 64, figs. 11–13.

non *Amplexopora chapparsi* (Loeblich). MERIDA AND BOARDMAN, 1967, Pl. 100, fig. 2.

*Description.*—Irregularly shaped, slightly elevated maculae present. Most zooecia develop mesozooecial stage in early ontogeny. Surface angles high (mean = 79.1°). Endozones thin (mean = 3.26 mm); exozones thick (mean = 0.88 mm); zoarial branches wide (mean = 5.02 mm); axial ratios small (mean = 0.65); mean autozooecial living chamber cross-sectional area in exozone 0.040 mm$^2$; mean autozooecial living chamber depth 0.330 mm; assuming cylindrical shape for autozooecial living chambers, mean volume 0.013 mm$^3$; mean autozooecial wall thickness in exozone 0.050 mm. Autozooecial basal diaphragms intersect walls at varying angles; shape usually planar, convex, or cystoidal, occasionally concave; mean spacing 1–13 per mm. Mean number of diaphragms 7.7/mm in mesozooecial stage of early ontogeny, decreasing to 1.4 in remaining endozone, increasing in exozone to 8.4. Autozooecial and mesozooecial walls in endozone straight or crenulated. Acanthostyles abundant (mean = 25.6/mm$^2$), small, and occur only in corners of adjacent autozooecia. (All qualitative character states are listed in Appendix 1 and quantitative data are summarized in Appendix 8.)

*Discussion.*—Ulrich (1893, p. 296) recognized the presence of a mesozooecial stage in early zooecial ontogeny in *Bimuropora winchelli* when he wrote, "in the attenuate proximal ends of the tubes the diaphragms are always closer than after the tubes have attained their full size." *Batostoma chapparsi* Loeblich, 1942, is considered conspecific with *Bimuropora winchelli* because the morphologic variation exhibited within colonies of *B. winchelli* incorporates the morphology of *Batostoma chapparsi* Loeblich, 1942. The discriminant analysis discussed earlier grouped Loeblich's (1942) holotype of *Batostoma chapparsi* with the other colonies of *Bimuropora winchelli*. This statistical test indicates that for the characters measured there are no significant morphological differences between the two species. Loeblich (1942) considered these two species as distinct solely on the basis of the abundance of autozooecial diaphragms. In his type material of both species, this character varies greatly. Also, the type specimens Loeblich designated for the two species were from the same geographic and stratigraphic locality and, thus, probably coexisted.

*Bimuropora winchelli* differs from most species of *Bimuropora* in having large zoarial branch diameters and thick exozones made of straight walled autozooecia.

*Material.*—The following material was measured and/or figured: lectotype USNM 43815 (herein designated for a colony of *Amplexopora winchelli* from Ulrich's 1886 type suite that he also figured as *Batostoma winchelli* in 1893, Pl. 27, fig. 2); paralectotypes USNM 435432–435435 (herein designated for colonies of *A. winchelli* from Ulrich's 1886 type suite); USNM 114566 (Loeblich's holotype of *Batostoma chapparsi*); hypotype USNM 114572 (Loeblich's hypotype of *Batostoma winchelli*); hypotypes USNM 435436–435447.

*Occurrence.*—*Bimuropora winchelli* has been reported in the Bromide Formation in Oklahoma (Loeblich, 1942), the "middle third of the Trenton Shales" (Decorah Formation) in southeast Minnesota (Ulrich, 1893), the Sprechts Ferry and Guttenberg Formations in Illinois, Wisconsin, and Iowa (Perry, 1962; Bork and Perry, 1967), the Logana and Jessamine Limestones in central Kentucky (Brown, 1965), the Denmark and Cobourg Formations in northeast New York (Ross, 1969), the Lower Chickamauga Group in northeast Alabama (McKinney, 1971), the Leray Formation in Canada (Wilson, 1921), and possibly from Estonia (Bassler, 1911). In Oklahoma specimens were found immediately below the Corbin Ranch Submember in the Pooleville Member of the Bromide Formation. These occurrences place the range of the species in the Blackriveran, Rocklandian, and Kirkfieldian Stages (Ross et al., 1982). Oklahoma specimens came from USNM localities 2132X$_{11}$, X$_{13}$, X$_{15}$, and 2189. Loeblich's type material of *Batostoma winchelli* and *Batostoma chapparsi* came from locality 2189, which is geographically and stratigraphically equivalent to 2132X.

### Genus CHAMPLAINOPORA Ross, 1970

*Atactotoechus* Duncan. Ross, 1963, p. 734.

*Champlainopora* Ross, 1970, p. 374.

*Type species.*—*Atactotoechus chazyensis* Ross, 1963, p. 734–737, Pl. 107, figs. 6–10, Pl. 108, figs. 1–11. Ross (1963) placed two new species (*A. chazyensis* and *A. kayi*) from the Middle Ordovician of New York into the upper Paleozoic genus *Atactotoechus* Duncan. Ross later reassigned them to a new genus *Champlainopora* making *A. chazyensis* the type species (Ross, 1970).

*Description.*—Maculae present in some species, composed of a cluster of megazooecia and mesozooecia. Zooecial arrangement ordered with initial buds developing from long, large, axial zooecia; zooecia have different lengths as a result of ordered zooecial arrangement; long, axial zooecia have larger diameters than other zooecia. Secondary zooecia bud from axial zooecia; secondary zooecia normal diameter but shorter than axial zooecia; tertiary zooecia bud from secondary zooecia, even shorter. Growth pattern evident in longitudinal section as large, long zooecia extending down axis of branch. Zooecial cross-sectional shape changing in conjunction with ontogenetic progression from polygonal to subpolygonal, growth pattern evident in transverse section: in center of endozone, mostly large subpolygonal zooecia; in outer endozone, mostly small polygonal zooecia. Endozones narrow, axial ratios small. Autozooecial wall boundary in exozone straight or irregular; autozooecial walls in exozone thick; autozooecial basal diaphragm shape planar, concave, convex, or cystoidal; spacing variable. Zooecial walls in endozone straight or wavy. Acanthostyles present or absent.

*Discussion.*—In the revised diagnosis of *Champlainopora*, Ross (1970, p. 374) noted the presence of small pores occurring at the zooecial wall boundaries. These pores are here referred to as pustules. In the colonies of the type species, the pustules are only locally developed. The pustules are lacking in the other species (*C. kayi*) that Ross assigned to the genus. Thus, pustules are not diagnostic of the genus as a whole.

The presence of large elongate axial zooecia in *Champlainopora* is similar to that of *Eridotrypa* Ulrich, 1893. Based on this, Astrova (1978) placed *C. chazyensis* (Ross, 1963) and *C. kayi* (Ross, 1963) in genus *Eridotrypa* (Ulrich, 1893). Pushkin also recognized this similarity and placed the two genera in the same family (Trematoporidae) but kept the genera distinct (Ro-

pot and Pushkin, 1987). The new material examined in this study supports Astrova's and Pushkin's observations that the axial zooecia in the two genera are similar. Based on a comparison of the material in this study with the type material of *Champlainopora* and *Eridotrypa,* the synonymization of these two genera cannot be supported. Nor should they be placed in the same family. Unlike *Champlainopora,* the constituent species of *Eridotrypa* (Ulrich, 1893) bud new zooecia intrazooecially and lack diaphragms in early zooecial ontogeny (McKinney, 1977).

*Champlainopora kayi* (Ross, 1963) is another matter. It is quite different from *C. chazyensis* because it lacks diaphragms in early zooecial ontogeny. It is herein removed from *Champlainopora.*

Based on the above description, the following species are herein assigned to *Champlainopora*: *Atactotoechus chazyensis* Ross, 1963; *Hallopora pachymura* Loeblich, 1942; *C. ramusculus* n. sp.; *C. arbucklensis* n. sp. Pushkin recently described the new species *Champlainopora oepiki* Pushkin, 1987 (Ropot and Pushkin, 1987). Having not seen the type material, its placement within *Champlainopora* cannot be confirmed.

For differences between *Champlainopora* and *Bimuropora,* see the comparisons section of *Bimuropora.*

*Occurrence.*—Species of *Champlainopora* have been reported in New York (Ross, 1963), Oklahoma (Loeblich, 1942), and possibly White Russia (Ropot and Pushkin, 1987). These occurrences place the range of the genus in the Chazyan Stage and the lower part of the Blackriveran Stage of the Middle Ordovician.

### CHAMPLAINOPORA CHAZYENSIS (Ross, 1963)
Figures 9.6–9.9, 10.1–10.3

*Atactotoechus chazyensis* Ross, 1963, p. 734–737, Pl. 107, figs. 6–10, Pl. 108, figs. 1–11.

*Description.*—Maculae and megazooecia absent. All zooecia develop mesozooecial stage in early ontogeny. Mean surface angle 63.8°; mean endozone diameter 1.42 mm; mean exozone width 0.49 mm; mean zoarial branch diameter 2.39 mm; mean axial ratio 0.59; mean autozooecial living chamber cross-sectional area in exozone 0.021 mm$^2$; mean living chamber depth 0.286 mm; assuming cylindrical shape for autozooecial living chambers, mean volume 0.006 mm$^3$. Integrate autozooecial wall structure in exozone locally disrupted by small pustules; when pustules absent autozooecial wall boundaries irregular or straight; autozooecial walls thicken greatly through exozone (mean = 0.115 mm) pinching out most mesozooecia and partially filling in autozooecial apertures. Autozooecial basal diaphragms intersect walls at varying angles; shape usually planar, convex, or cystoidal, occasionally concave; mean spacing 1–19 per mm. Mean number of diaphragms per mm in mesozooecial stage of early ontogeny 8.9, decreasing to 3.0 in remaining endozone, increasing in exozone to 9.9. Autozooecial and mesozooecial walls in endozone wavy. Acanthostyles absent. (All qualitative character states are listed in Appendix 1 and quantitative data are summarized in Appendix 9.)

*Discussion.*—Ross (1963, p. 735; 1970, p. 374) noted the presence of pustules at the zooecial wall boundaries. They are locally developed both laterally and vertically within the exozone. Where they occur they are commonly in great abundance and disrupt the wall laminae. As zooecial ontogeny progresses through the exozone, zooecial walls thicken, causing the pustules and smaller mesozooecia to pinch out. Simultaneously, the smaller mesozooecia become filled in as their walls thicken to the point of completely or partially closing the apertures. When the pustules are absent, or in the outer part of a thick exozone, the zooecial wall boundaries are not disrupted and are marked by a distinct line that is either crenulated or straight.

*Champlainopora chazyensis* differs from all other species of *Champlainopora* in having pustules developed along the zooecial boundaries that disrupt the wall laminae and in having thick autozooecial walls in the exozone that commonly fill in the apertures.

*Material.*—The following material was measured and/or figured: holotype YPM 22249 (Ross' holotype of *Atactotoechus chazyensis*); paratypes YPM 22246, 22248, 22256, 22265 (Ross' paratypes of *A. chazyensis*); hypotypes USNM 435448–435467.

*Occurrence.*—*Champlainopora chazyensis* has been reported

→

FIGURE *10—1–3, Champlainopora chazyensis* (Ross). *1,* zooecial wall thickening in exozone, crenulated integrate wall boundaries with pustules, USNM 435453, USNM locality 2115B, longitudinal section, ×100; *2,* growth pattern with long, large, axial zooecium budding off shorter, smaller secondary zooecia which then budded off even shorter tertiary zooecia, wavy zooecial walls in endozone, USNM 435455, USNM locality 2129N, longitudinal section, ×30; *3,* zooecial wall thickening in exozone, crenulated integrate wall boundaries, planar autozooecial basal diaphragms, mesozooecium at bottom pinching out due to wall thickening, USNM 435466, USNM locality 2153Z, longitudinal section, ×100. *4–9, Champlainopora ramusculus* n. sp. *4,* large subpolygonal axial zooecia surrounded by smaller polygonal zooecia, small circular zoarial branch cross-sectional shape, USNM 435475, USNM locality 2132E, transverse section, ×30; *5,* oval autozooecial apertures in exozone, mesozooecia at corners of adjacent autozooecia, USNM 435478, USNM locality 2132E, tangential section, ×50; *6,* growth pattern with long, large, axial zooecium budding off shorter smaller secondary zooecia which then budded off even shorter tertiary zooecia, thin endozone, thin exozone, low surface angle, USNM 435472, USNM locality 2132E, longitudinal section, ×30; *7,* growth pattern with closely spaced diaphragms in early zooecial ontogeny and widely spaced diaphragms in later ontogeny, USNM 435473, USNM locality 2132E, longitudinal section, ×30; *8,* remnant growing tip in endozone, USNM 435470, USNM locality 2116B, longitudinal section, ×50; *9,* zooecial wall thickening in exozone, crenulated integrate wall boundary, cystoidal autozooecial basal diaphragms, USNM 435468, USNM locality 2132E, longitudinal section, ×100.

FIGURE *11—1–7, Champlainopora pachymura* (Loeblich). *1,* large, subpolygonal axial zooecia surrounded by smaller, polygonal zooecia, USNM 435484, USNM locality 2116D, transverse section, ×30; *2,* elevated macula with megazooecia and mesozooecia, USNM 435484, USNM locality 2116D, longitudinal section, ×30; *3,* remnant growing tip in endozone, USNM 435489, USNM locality 2116D, longitudinal section, ×50; *4,* zooecial wall thickening in exozone, straight integrate wall boundary, cystoidal autozooecial basal diaphragms, USNM 435482, USNM locality 2116D, longitudinal section, ×100; *5,* subpolygonal autozooecial apertures in exozone, six-sided polygonal zooidal cross-sectional shapes, integrate wall structure, macular mesazooecia and mesozooecia in lower left, USNM 435482, USNM locality 2116D, tangential section, ×30; *6,* growth pattern with closely spaced diaphragms in early zooecial ontogeny and widely spaced diaphragms in later ontogeny, USNM 435482, USNM locality 2116D, longitudinal section, ×30; *7,* growth pattern with long, large, axial zooecium budding off shorter, smaller secondary zooecia which then budded off even shorter tertiary zooecia, USNM 435482, USNM locality 2116D, longitudinal section, ×30.


1

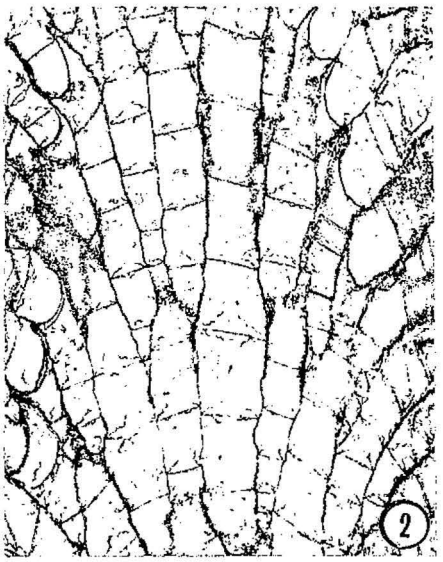
2


3

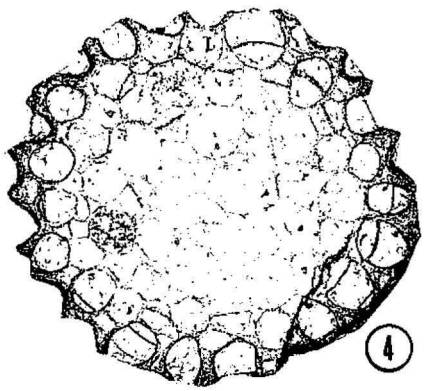
4

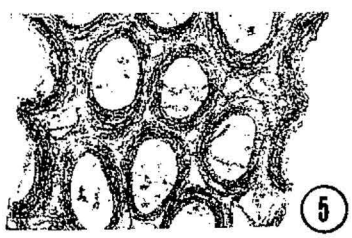
5

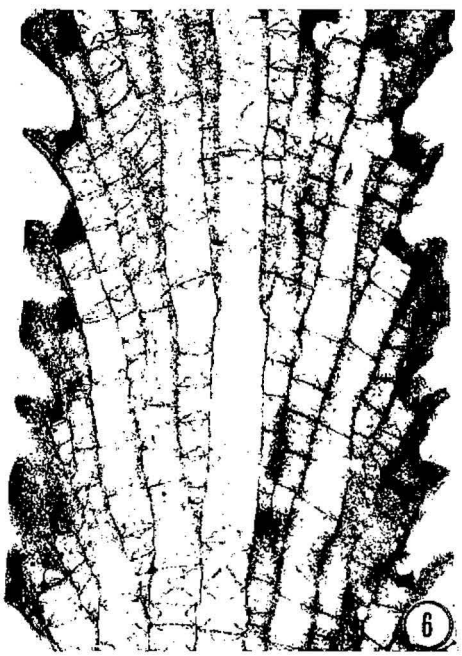
6

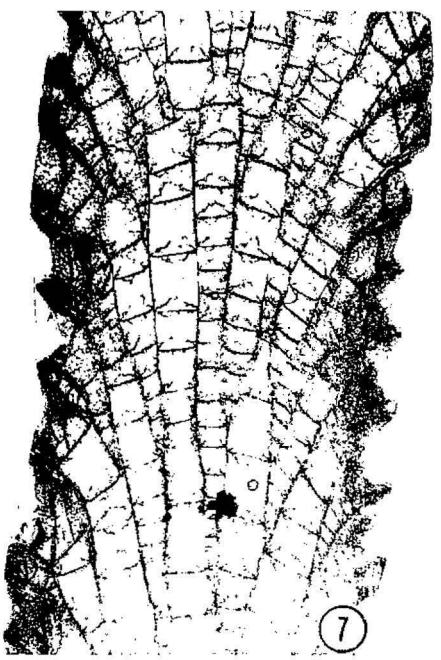
7

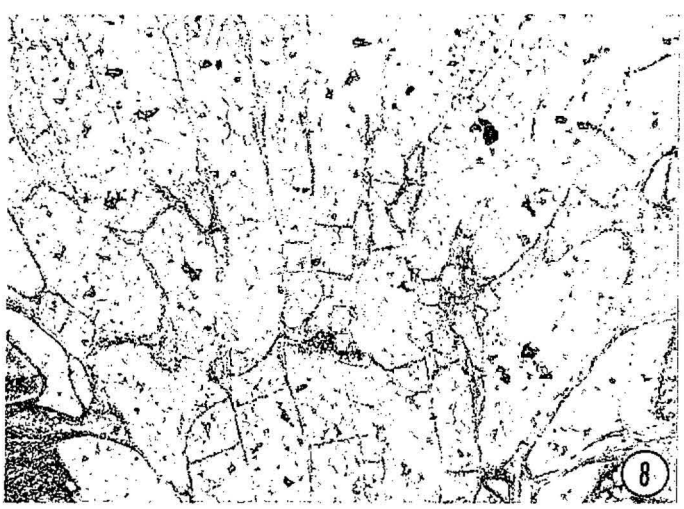
8

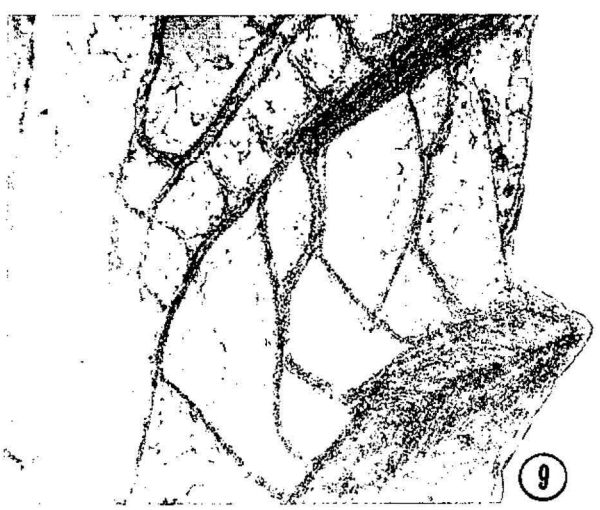
9

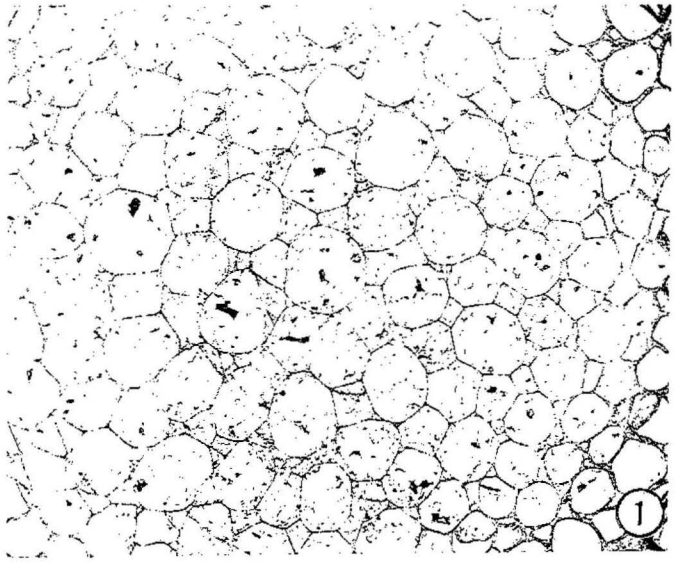
1

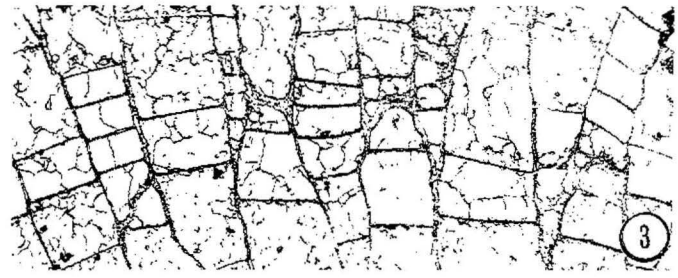
3

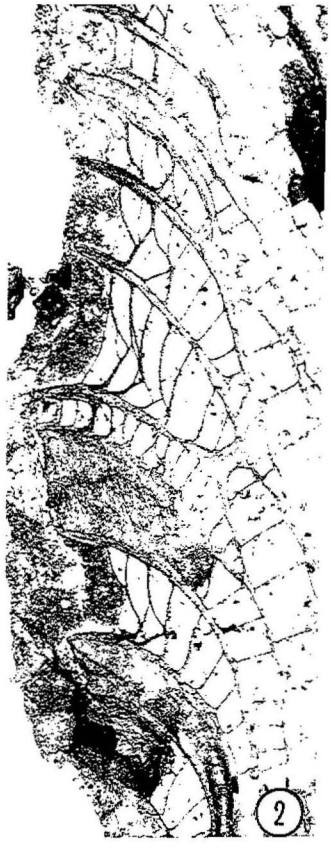
2


5


4

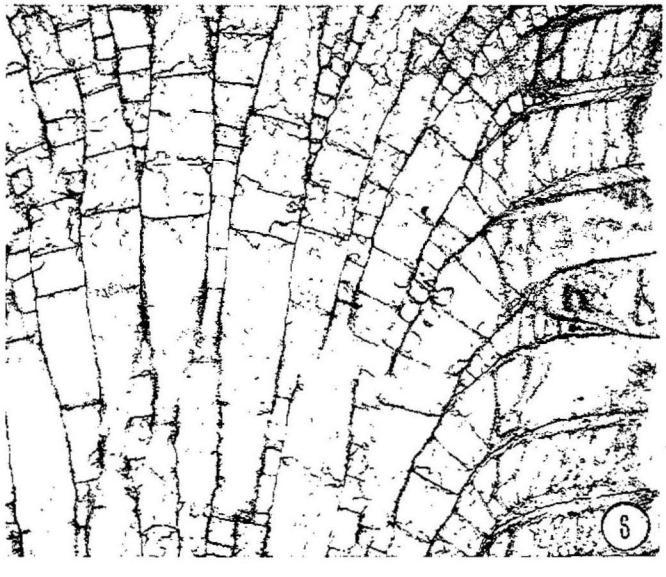
6

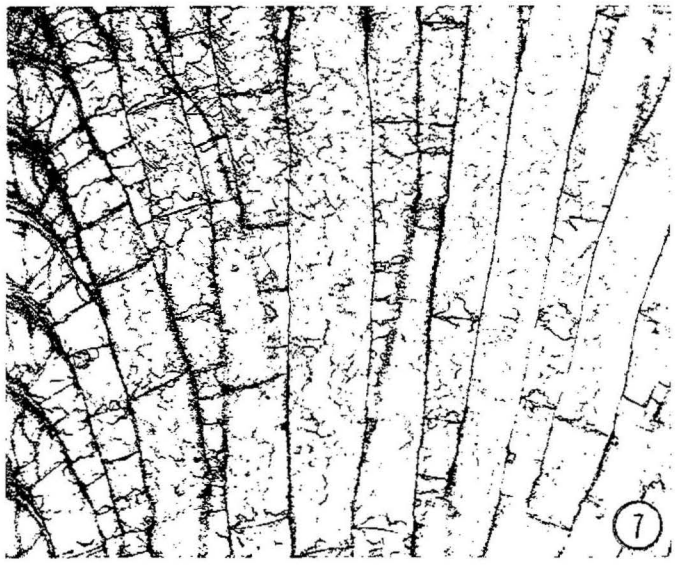
7

in the Chazy Formation (Day Point, Crown Point, and Valcour Limestones) in northeast New York and northwest Vermont (Ross, 1963). In Oklahoma specimens were found in the McLish and Tulip Creek Formations. These occurrences place the range of the species in the Chazyan Stage (Ross et al., 1982). Oklahoma specimens came from USNM localities 2114E, F, $G_1$, $G_2$, G; 2115A, B; 2129$M_1$, N; 2130B, D, E; 2153P, S, W, Z, and AA.

### CHAMPLAINOPORA RAMUSCULUS n. sp.
Figure 10.4–10.9

*Etymology.*—The name is derived from *ramus*, the Latin noun for branch. The diminutive form is *ramusculus*. This is in reference to the small zoarial branches indicative of the species.

*Diagnosis.*—*Champlainopora* with maculae absent; low surface angle; narrow endozone; thin exozone; narrow branches; small axial ratio; small, oval autozooecial living chamber cross sections in exozone; shallow autozooecial living chambers in exozone; acanthostyles absent.

*Description.*—Maculae and megazooecia absent. All zooecia develop mesozooecial stage in early ontogeny. Surface angles low (mean = 60.3°); endozones narrow (mean = 1.02 mm); exozones thin (mean = 0.33 mm); zoarial branches narrow (mean = 1.67 mm); axial ratios small (mean = 0.60); autozooecial living chamber cross-sectional shapes oval, areas small (mean = 0.025 mm$^2$), living chambers shallow (mean = 0.269 mm); assuming cylindrical shape for autozooecial living chambers, mean volume 0.007 mm$^3$. Autozooecial wall boundaries in exozone irregular; mean autozooecial wall thickness in exozone 0.079 mm. Autozooecial basal diaphragms intersect walls at varying angles; shape usually planar, convex, or cystoidal, occasionally concave or S-shaped; mean spacing 0–24 per mm. Mean number of diaphragms per mm in mesozooecial stage of early ontogeny 9.3, decreasing to 2.4 in remaining endozone, increasing in exozone to 12.0. Autozooecial and mesozooecial walls in endozone generally straight. Acanthostyles absent. (All qualitative character states are listed in Appendix 1 and quantitative data are summarized in Appendix 10.)

*Discussion.*—*Champlainopora ramusculus* differs from all other species of *Champlainopora* in having low surface angles, thin endozones, exozones, and zoarial branches, shallow autozooecial living chambers, and a lack of maculae and megazooecia. In some of these respects, *C. ramusculus* is similar to species of *Eridotrypa*. The two can be readily distinguished by their budding patterns. *Champlainopora ramusculus* exhibits an interzooidal pattern while species of *Eridotrypa* exhibit an intrazooidal pattern.

*Material.*—The following material was measured and/or figured: holotype USNM 435468; paratypes USNM 435469–435481.

*Occurrence.*—Specimens of *Champlainopora ramusculus* were found in the lower part of the Mountain Lake Member of the Bromide Formation. This places the range of the species in the lowermost part of the Blackriveran Stage (Ross et al., 1982). Specimens came from USNM localities 2116B and 2132E.

### CHAMPLAINOPORA PACHYMURA (Loeblich, 1942)
Figure 11.1–11.7

*Hallopora pachymura* LOEBLICH, 1942, p. 431, Pl. 62, figs. 12–14.

*Description.*—Irregularly shaped, elevated maculae present. All zooecia develop mesozooecial stage in early ontogeny. Mean surface angle 69.6°; mean endozone diameter 2.60 mm; mean exozone width 0.65 mm; mean zoarial branch diameter 3.90 mm; mean axial ratio 0.67; autozooecial living chamber cross-sectional areas large (mean = 0.045 mm$^2$); mean autozooecial living chamber depth 0.300 mm; assuming cylindrical shape for autozooecial living chambers, mean volume 0.014 mm$^3$. Autozooidal boundary cross-sectional shapes in exozone generally hexagonal; autozooecial wall boundaries in exozone straight; autozooecial walls thicken through exozone (mean = 0.081 mm) pinching out most mesozooecia. Autozooecial basal diaphragms intersect walls at varying angles; shape usually planar, convex, or cystoidal, occasionally concave or S-shaped; mean spacing 0–16 per mm. S-shaped and cystoidal autozooecial basal diaphragms have their more distal end (relative to zooecium) located on distal side of zooecium (relative to colony). Mean number of diaphragms per mm in mesozooecial stage of early ontogeny 9.1, decreasing to 2.4 in remaining endozone, increasing in exozone to 9.6. Autozooecial and mesozooecial walls in endozone generally straight. Acanthostyles absent. (All qualitative character states are listed in Appendix 1 and quantitative data are summarized in Appendix 11.)

*Discussion.*—*Champlainopora pachymura* differs from all other species of *Champlainopora* in having very straight autozooecial wall boundaries in the exozone, abundant cystoidal autozooecial basal diaphragms in the exozone, large autozooecial living chamber cross-sectional areas, hexagonal autozooidal boundary cross sections in the exozone, and large megazooecia.

*Material.*—The following material was measured and/or figured: holotype USNM 114604 (Loeblich's holotype of *Hallopora pachymura*); paratype USNM 100482 (Loeblich's paratype of *H. pachymura*); hypotypes USNM 435482–435496.

*Occurrence.*—*Champlainopora pachymura* has been reported only in the Bromide Formation in Oklahoma (Loeblich, 1942). Specimens were found in the middle and upper parts of the Mountain Lake Member of the Bromide Formation. This places the range of the species in the lower part of the Blackriveran Stage (Ross et al., 1982). Specimens came from USNM localities 2116D, 2155U, 2184, 2211, and 38974-1. Localities 2184 of Loeblich and 38974-1 of the author are geographically and stratigraphically equivalent to 2116D. Loeblich's type material of *Hallopora pachymura* came from locality 2211, which is geographically and stratigraphically equivalent to 2116D.

→

FIGURE *12—1–9, Champlainopora arbucklensis* n. sp. *1,* subpolygonal autozooecial apertures in exozone, abundant acanthostyles, USNM 435506, USNM locality 2116$A_1$, tangential section, ×50; *2,* remnant growing tip in endozone, USNM 435514, USNM locality 2116A, longitudinal section, ×50; *3,* first autozooecial basal diaphragms in exozone very thick, high surface angle, USNM 435515, USNM locality 2116A, longitudinal section, ×30; *4,* growth pattern with long, large, axial zooecium budding off shorter smaller secondary zooecia which then budded off even shorter tertiary zooecia, USNM 435497, USNM locality 2116$A_1$, longitudinal section, ×30; *5,* large subpolygonal axial zooecia surrounded by smaller polygonal zooecia, USNM 435513, USNM locality 2116A, transverse section, ×30; *6,* macula near bottom with megazooecia and mesozooecia, integrate wall structure, USNM 435501, USNM locality 2116$A_1$, tangential section, ×30; *7,* growth pattern with closely spaced diaphragms in early zooecial ontogeny and widely spaced diaphragms in later ontogeny, USNM 435505, USNM locality 2116$A_1$, longitudinal section, ×30; *8,* zooecial wall thickening in exozone, crenulated integrate wall boundaries, acanthostyles, thick exozone, thick zooecial walls, USNM 435510, USNM locality 2116$A_1$, longitudinal section, ×50; *9,* autozooecial apertures almost completely filled in due to very thick zooecial walls, USNM 435499, USNM locality 2116$A_1$, tangential section, ×30.

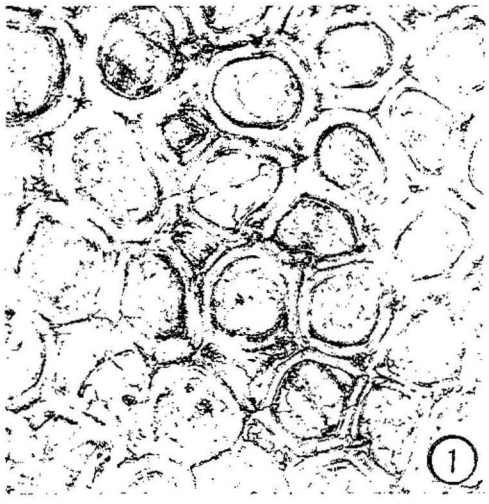
1


2


3

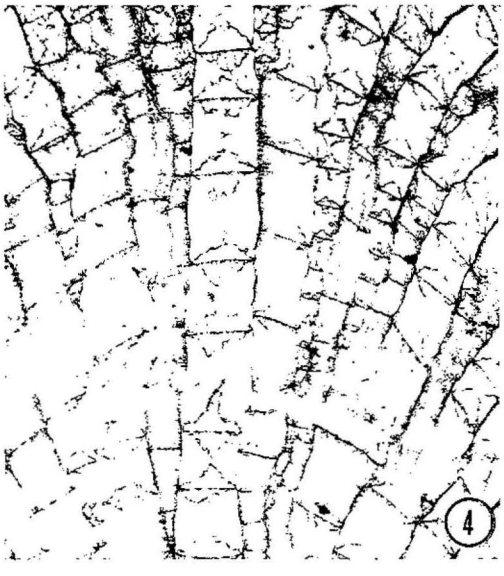
4

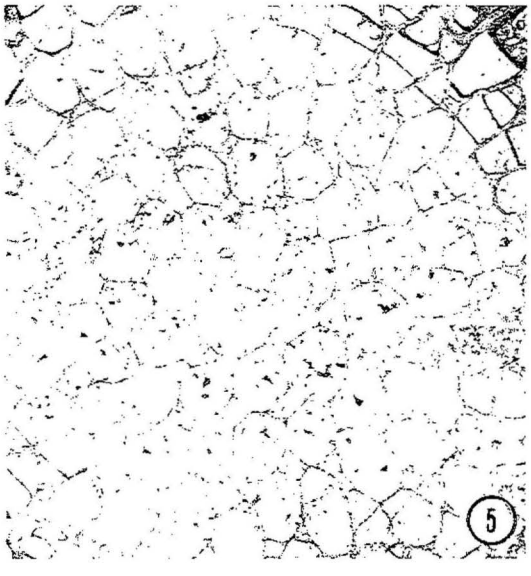
5

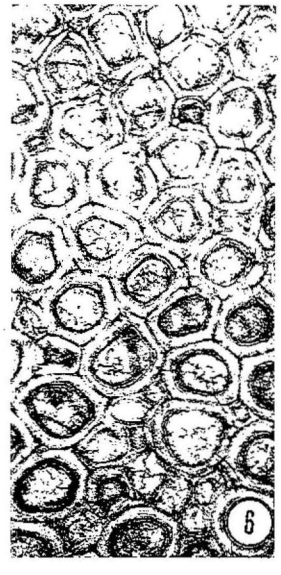
6

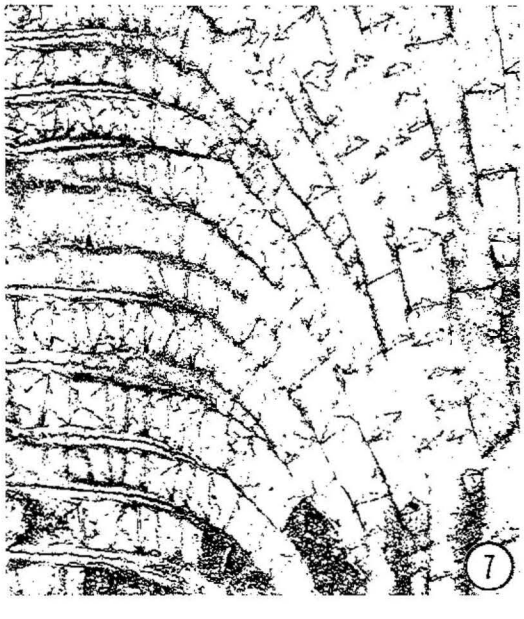
7

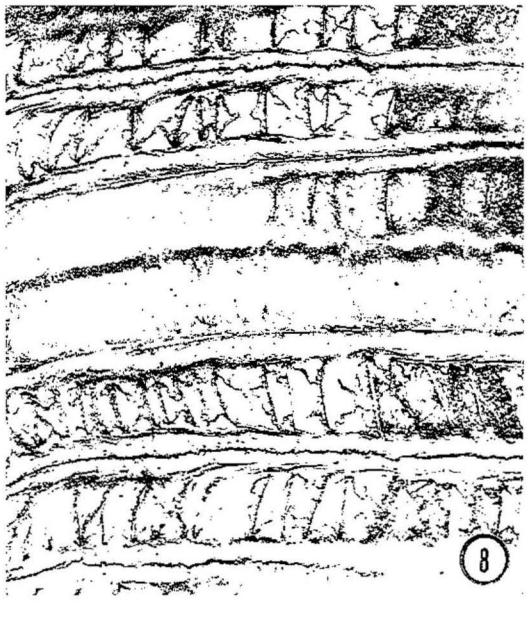
8


9

CHAMPLAINOPORA ARBUCKLENSIS n. sp.
Figure 12.1–12.9

*Etymology.*—The name is derived from the Arbuckle Mountains where this species was found.

*Diagnosis.*—*Champlainopora* with maculae present; high surface angle; thick exozone; small autozooecial living chamber cross-sectional areas in exozone; deep autozooecial living chambers in exozone; thick autozooecial walls in exozone cause some mesozooecia to pinch out; first autozooecial basal diaphragm in exozone S-shaped and thickened; cystoidal diaphragms common at zooecial bend from endozone to exozone; acanthostyles common.

*Description.*—Irregularly shaped, slightly elevated maculae. All zooecia develop mesozooecial stage in early ontogeny. Surface angles high (mean = 83.5°); mean endozone diameter 2.38 mm; exozones thick (mean = 1.15 mm); mean zoarial branch diameter 4.67 mm; mean axial ratio 0.52; autozooecial living chamber cross-sectional areas small (mean = 0.024 mm$^2$), living chambers deep (mean = 0.391 mm); assuming cylindrical shape for autozooecial living chambers, mean volume 0.009 mm$^3$. Autozooecial wall boundaries in exozone irregular; autozooecial walls thicken through exozone (mean = 0.102 mm) pinching out most mesozooecia and partially filling in autozooecial apertures. Autozooecial basal diaphragms intersect walls at varying angles; shape usually planar, convex, or cystoidal, occasionally concave or S-shaped; mean spacing 1–12 per mm. First autozooecial basal diaphragm in exozone usually S-shaped and thick. Cystoidal diaphragms abundant at zooecial bend. Mean number of diaphragms per mm in mesozooecial stage of early ontogeny 9.2, decreasing to 2.3 in remaining endozone, increasing in exozone to 8.5. Autozooecial and mesozooecial walls in endozone generally straight. Acanthostyles abundant (mean = 26.2 per mm$^2$), well defined, surround autozooecia but do not inflect walls. (All qualitative character states are listed in Appendix 1 and quantitative data are summarized in Appendix 12.)

*Discussion.*—*Champlainopora arbucklensis* n. sp. differs from all other species of *Champlainopora* in having high surface angles, thick exozones, thick autozooecial walls in the exozone that commonly fill in the apertures, thick S-shaped first exozonal autozooecial basal diaphragms, and abundant cystoidal autozooecial basal diaphragms at zooecial bend.

*Material.*—The following material was measured and/or figured: holotype USNM 435497; paratypes USNM 435498–435515.

*Occurrence.*—Specimens of *Champlainopora arbucklensis* were found in the lower and middle parts of the Mountain Lake Member of the Bromide Formation. This places the range of the species in the uppermost part of the Chazyan Stage and the lower part of the Blackriveran Stage (Ross et al., 1982). Specimens came from USNM localities 2116A, $A_1$; 2132E; and 2155L.

ACKNOWLEDGMENTS

I thank R. Boardman, W. Hartman, O. Karklins, J. Pachut, J. Ross, D. Schindel, and E. Vrba for reviewing earlier drafts of this manuscript; the U.S. National Museum of Natural History's Department of Paleobiology for office space and access to type specimens, collections, and laboratory facilities; A. Cheetham and L.-A. Hayek for assistance with statistical analyses; D. Dean for assistance with specimen preparation; V. Funk for assistance with phylogenetic analyses; and R. White for loaning Yale Peabody Museum type specimens. This research was made possible by funding from Yale University, Atlantic Richfield Foundation, The Woman's Seaman's Friend Society of Connecticut, Yale Peabody Museum Schuchert Fund, and grants from Sigma Xi and the Geological Society of America (#3804-87).

REFERENCES

ASTROVA, G. G. 1965. Morphology, evolutionary history, and systematics of Ordovician and Silurian bryozoans. Trudy Akademiya Nauk SSSR, Paleontologicheskiy Institut, Vol. 106, 432 p.

——. 1978. Historical development, systematics, and phylogeny of Bryozoa. Trudy Akademiya Nauk SSSR, Paleontologicheskiy Institut, Vol. 169, 240 p.

BASSLER, R. S. 1911. The early Paleozoic Bryozoa of the Baltic provinces. U.S. National Museum, Bulletin 77, 382 p.

BOARDMAN, R. S. 1960. Trepostomatous Bryozoa of the Hamilton Group of New York State. U.S. Geological Survey Professional Paper 340, 87 p.

——, A. H. CHEETHAM, AND P. L. COOK. 1970. Intracolony variation and the genus concept in Bryozoa. Proceedings of the North American Paleontological Convention, p. 294–320.

——, AND F. K. MCKINNEY. 1985. Soft part characters in stenolaemate taxonomy, p. 35–44. *In* C. Nielsen and G. P. Larwood (eds.), Bryozoa: Ordovician to Recent. Olsen and Olsen, Fredensborg, Denmark.

BORK, K. B., AND T. G. PERRY. 1967. Bryozoa (Ectoprocta) of Champlainian age (Middle Ordovician) from northwestern Illinois and adjacent parts of Iowa and Wisconsin. Part I. *Amplexopora, Monotrypella, Hallopora,* and *Batostoma.* Journal of Paleontology, 41:1365–1392.

BROWN, G. D., JR. 1965. Trepostomatous Bryozoa from the Logana and Jessamine Limestones (Middle Ordovician) of the Kentucky Bluegrass region. Journal of Paleontology, 39:974–1006.

CONTI, S., AND E. SERPAGLI. 1987. Functional morphology of the caplike apparatus in autozooids of a Palaeozoic trepostome bryozoan. Lethaia, 20:1–20.

COOPER, G. A. 1956. Chazyan and related brachiopods. Smithsonian Miscellaneous Collections, 127:1–1245.

CORYELL, H. N. 1921. Bryozoan faunas of the Stones River Group of central Tennessee. Proceedings of the Indiana Academy of Sciences, 1919:261–340.

DECKER, C. E., AND C. A. MERRITT. 1931. The stratigraphy and physical characteristics of the Simpson Group. Oklahoma Geological Survey Bulletin 55, 112 p.

FARMER, G. T., JR. 1974. The oldest well-preserved bryozoan fauna in the world? Oklahoma Geology Notes, 34:99–101.

——. 1975. New bifoliate tubular bryozoan genera from the Simpson Group (Middle Ordovician), Arbuckle Mountains, Oklahoma. Bulletins of American Paleontology, 67:123–138.

FRITZ, M. A. 1957. Bryozoa (mainly Trepostomata) from the Ottawa Formation (Middle Ordovician) of the Ottawa–St. Lawrence Lowland. Geological Survey of Canada Bulletin, 42:1–75.

HENDY, M. D., AND D. PENNY. 1982. Branch and bound algorithms to determine minimal evolutionary trees. Mathematical Biosciences, 59:277–290.

KANYGIN, A. V., A. M. OBUT, K. N. VOLKOVA, AND A. M. YAROSHINSKAYA. 1984. Phylum Bryozoa, p. 19–31. *In* T. Moskalenko (ed.), Ordovician of the Siberian Platform. Paleontological Atlas. U.S.S.R. Academy of Sciences, Siberian Division, Trudy of the Institute of Geology and Geophysics, Vol. 590.

LOEBLICH, A. R., JR. 1942. Bryozoa from the Ordovician Bromide Formation, Oklahoma. Journal of Paleontology, 16:413–436.

MCKINNEY, F. K. 1971. Trepostomatous Ectoprocta (Bryozoa) from the Lower Chickamauga Group (Middle Ordovician), Wills Valley, Alabama. Bulletins of American Paleontology, 60:195–337.

——. 1977. Autozooecial budding patterns in dendroid Paleozoic bryozoans. Journal of Paleontology, 51:303–329.

——, AND R. S. BOARDMAN. 1985. Zooidal biometry of Stenolaemata, p. 193–203. *In* C. Nielsen and G. P. Larwood (eds.), Bryozoa: Ordovician to Recent. Olsen and Olsen, Fredensborg, Denmark.

MERIDA, J. E., AND R. S. BOARDMAN. 1967. The use of Paleozoic Bryozoa from well cuttings. Journal of Paleontology, 41:763–765.

PERRY, T. G. 1962. Sprechts Ferry (Middle Ordovician) bryozoan fauna from Illinois, Wisconsin, and Iowa. Illinois State Geological Survey Circular 326, 36 p.

ROPOT, B. F., AND B. I. PUSHKIN. 1987. Ordovician of White Russia. Minsk, Nauka i Tekhnika, 234 p.
ROSS, J. R. P. 1963. Chazyan (Ordovician) leptotrypellid and atactotoechid bryozoa. Palaeontology, 5:727–739.
ROSS, J. P. 1964. Morphology and phylogeny of early Ectoprocta (Bryozoa). Geological Society of America Bulletin, 75:927–948.
——. 1967. Champlainian Ectoprocta (Bryozoa), New York State. Journal of Paleontology, 41:632–648.
——. 1969. Champlainian (Ordovician) Ectoprocta (Bryozoa), New York State, Part II. Journal of Paleontology, 43:257–284.
——. 1970. Distribution, paleoecology and correlation of Champlainian Ectoprocta (Bryozoa), New York State, Part III. Journal of Paleontology, 44:346–382.
ROSS, R. J., JR. 1976. Ordovician sedimentation in the western United States, p. 73–105. *In* M. G. Bassett (ed.), The Ordovician System. University of Wales Press, Cardiff.
——, ET AL. 1982. The Ordovician System in the United States. International Union of Geological Societies, Publication 12, 73 p.
SCHAFER, P. 1985. Significance of soft part morphology in the classification of recent tubuliporid cyclostomes, p. 273–284. *In* C. Nielsen and G. P. Larwood (eds.), Bryozoa: Ordovician to Recent. Olsen and Olsen, Fredensborg, Denmark.
SPRINKLE, J. 1982. Echinoderm faunas from the Bromide Formation (Middle Ordovician) of Oklahoma. University of Kansas, Paleontological Contributions, Monograph 1, University of Kansas Paleontological Institute, Lawrence, 369 p.
SPSS, INC. 1988. SPSS/PC+, Version 2.0. SPSS Inc., Chicago, Illinois.
SWOFFORD, D. L. 1985. PAUP: Phylogenetic Analysis Using Parsimony, Version 2.4. David L. Swofford, Champaign, Illinois.
——. 1986. CONTREE: Consensus Tree Program, Version 1/3/86. David L. Swofford, Champaign, Illinois.
ULRICH, E. O. 1882. American Paleozoic Bryozoa. Journal of the Cincinnati Society of Natural History, 5:121–175.
——. 1886. Report on the Lower Silurian Bryozoa with preliminary descriptions of some of the new species. Geological and Natural History Survey of Minnesota, Annual Report, 14:58–103.
——. 1893. The Bryozoa of the Lower Silurian in Minnesota. Geological and Natural History Survey of Minnesota, Final Report, 3: 96–332.
WILSON, A. E. 1921. The range of certain Lower Ordovician faunas of the Ottawa Valley with descriptions of some new species. Canada Geological Survey Bulletin, 33:19–57.
WINSTON, J. E. 1981. Feeding behavior of modern bryozoans, p. 1–21. *In* T. W. Broadhead (ed.), Lophophorates, Notes for a Short Course. University of Tennessee, Department of Geological Sciences, Studies in Geology, No. 5.

ACCEPTED 28 FEBRUARY 1990

## APPENDIX 1

*Character List*

SECTION

Longitudinal = L
Tangential = T
Transverse = R
Colony Surface = S

### SCORED MULTISTATE CHARACTERS

#### ZOARIUM CHARACTERS

1. Growth habit — L, S
   1) Variable
   2) Encrusting
   3) Massive/ramose
   4) Massive
   5) Ramose
2. Occurrence of intracolony overgrowths — L, S
   1) Absent
   2) Present
3. Branch cross-sectional shape — R
   1) Not applicable because growth habit is not ramose
   2) Subcircular to oval
   3) Circular
4. Surface angle — L
   1) 0–70°
   2) 71–78°
   3) 79–90°
5. Type of interzooidal budding — L, T
   1) Intrazooidal pattern (intrazooecial of McKinney, 1977)
   2) Interzooidal pattern (interzooecial of McKinney, 1977)
6. Zooidal arrangement — L, T
   1) Ordered
   2) Disordered
7. Occurrence of large, long, axial zooecia — L, T
   1) Present
   2) Absent
8. Number of diaphragms per mm in early zooidal ontogeny — L
   1) 0.0
   2) 0.1–9.0
   3) >9.0
9. Length of mesozooidal stage in early zooidal ontogeny — L
   1) Not applicable because no mesozooidal stage in early zooidal ontogeny
   2) <0.1 mm
   3) >0.1 mm
10. Occurrence of remnant growing tips in endozone — L
    1) Present
    2) Absent
11. Occurrence of a line of distally concaved diaphragms probably formed after an environmental perturbation and before normal growth resumed — L
    1) Absent
    2) Present
12. Diaphragms present in zooids at nearly the same level over a moderately large area of endozone and then pass into exozone — L
    1) No
    2) Yes
13. Macular topography — L, S
    1) Not applicable because maculae absent
    2) Flat
    3) Depressed
    4) Elevated
14. Macular shape — T, S
    1) Not applicable because maculae absent
    2) Irregular
    3) Circular
    4) Elongate
    5) Stellar

#### AUTOZOOID CHARACTERS (scored between maculae)

15. Living chamber cross-sectional shape in endozone — R
    1) Ontogenetically changes from polygonal to subpolygonal as each zooid comes into contact with more adjacent zooids
    2) Ontogenetically changes from polygonal to subpolygonal to subcircular to circular as each zooid comes into contact with more adjacent zooids
16. Living chamber cross-sectional shape in outer exozone — T
    1) Petaloid (inflected by acanthostyles)
    2) Oval
    3) Circular
    4) Subcircular
    5) Circular to subpolygonal
    6) Subpolygonal
    7) Polygonal

17. Zooidal boundary cross-sectional shape in outer exozone T
    1) Oval
    2) Circular
    3) Subcircular
    4) Subpolygonal
    5) Polygonal

18. Wall shape in endozone where autozooecia and mesozooecia adjacent L
    1) Regular
    2) Wavy
    3) Crenulated
    4) Fluted

19. Wall structure in exozone L, T
    1) Microcrystalline
    2) Sharp, distinct, integrate
    3) Merged, indistinct, amalgamate

20. Shape of wall boundary in exozone L
    1) Microcrystalline
    2) Irregular
    3) Straight
    4) Not applicable because wall boundary is not integrate

21. Wall laminae configuration in exozone L
    1) Unknown because laminae indistinct
    2) Sharply convex (V-shaped) distally
    3) Broadly convex (U-shaped) distally

22. Occurrence of planar-shaped diaphragms in exozone L
    1) Absent (0%)
    2) Rare (1–25%)
    3) Common (26–75%)
    4) Abundant (>75%)

23. Occurrence of distally concave-shaped diaphragms in exozone L
    1) Absent (0%)
    2) Rare (1–25%)
    3) Common (26–75%)
    4) Abundant (>75%)

24. Occurrence of distally convex-shaped diaphragms in exozone L
    1) Absent (0%)
    2) Rare (1–25%)
    3) Common (26–75%)
    4) Abundant (>75%)

25. Occurrence of S-shaped diaphragms in exozone L
    1) Absent (0%)
    2) Rare (1–25%)
    3) Common (26–75%)
    4) Abundant (>75%)

26. Occurrence of cystoidal diaphragms in exozone L
    1) Absent (0%)
    2) Rare (1–25%)
    3) Common (26–75%)
    4) Abundant (>75%)

27. Angle at which exozonal diaphragms intersect walls L
    1) Roughly 90°
    2) Less than or greater than 90°
    3) Variable

28. More distal side of basal diaphragms in exozonal autozooids L
    1) Usually on proximal side of zooid (75–100%)
    2) On distal or proximal side of zooid (26–74%/26–74%)
    3) Usually on distal side of zooid (75–100%)

29. Occurrence of autozooidal wall thickening by diaphragms (diaphragm-wall unit of Boardman, 1960) in exozone L
    1) Neither (no noticeable thickening)
    2) Usually proximal (75–100%)
    3) Distal and proximal (26–74%/26–74%)
    4) Usually distal (75–100%)

MEGAZOOID CHARACTERS (scored in maculae)

30. Occurrence in exozone T
    1) Absent
    2) Present

31. Location of origination L
    1) Not applicable because megazooids absent
    2) Not applicable because no distinction between endozone and exozone
    3) In outer endozone
    4) At endozone/exozone boundary
    5) In exozone

32. Living chamber cross-sectional shape in outer exozone T
    1) Not applicable because megazooids absent
    2) Oval
    3) Circular
    4) Subcircular
    5) Subpolygonal
    6) Polygonal

MESOZOOID CHARACTERS (scored between maculae)

33. Occurrence in relation to autozooids in outer exozone T
    1) Absent
    2) Only in corners of adjacent autozooids
    3) In and between corners of adjacent autozooids
    4) In and between corners and nearly or completely isolate autozooids

34. Location of origination L
    1) Not applicable because no distinction between endozone and exozone
    2) In outer endozone
    3) At endozone/exozone boundary
    4) In exozone

35. Shape of diaphragms in exozone L
    1) Slightly curved and distally concave
    2) Planar
    3) Slightly curved and distally convex

36. Angle at which exozonal diaphragms intersect walls L
    1) Roughly 90°
    2) Less than and greater than 90°

37. Zooidal boundary cross-sectional shape in outer exozone T
    1) Oval
    2) Circular
    3) Subcircular
    4) Subpolygonal
    5) Polygonal

ACANTHOSTYLE CHARACTERS (scored between maculae)

38. Occurrence in outer exozone T
    1) Absent
    2) Only in corners of adjacent zooids
    3) Surround zooids but do not inflect walls
    4) Surround zooids and inflect walls

39. Location of origination L
    1) Not applicable because acanthostyles absent
    2) Endozone
    3) Endozone/exozone boundary
    4) Exozone

40. Microstructure L
    1) Not applicable because acanthostyles absent
    2) Sharply convex (V-shaped) distally laminae with core of clear calcite
    3) Broadly convex (U-shaped) distally laminae with core of clear calcite

MEASURED CHARACTERS
(measured in mm unless otherwise indicated)

ZOARIUM CHARACTERS

41. Surface angle (in degrees) L
42. Endozone diameter L
43. Exozone width L
44. Calculated branch diameter (#42 + 2*#43)
45. Calculated axial ratio (#42/#44)

AUTOZOOID CHARACTERS (measured between maculae)

46. Area of living chamber cross section in outer exozone T
47. Calculated diameter of living chamber cross section in outer exozone ($2*[\#46/3.14]^{.5}$)
48. Outermost living-chamber depth L
49. Distance between adjacent living chamber (i.e., wall thickness) in outer exozone T

COUNTED CHARACTERS

AUTOZOOID CHARACTERS (counted between maculae)

50. Number of diaphragms per mm in early ontogeny L
51. Number of diaphragms per mm in rest of endozone L
52. Number of diaphragms per mm in exozone L

MESOZOOID CHARACTERS (counted between maculae)

53. Number of diaphragms per mm in exozone L
54. Number of complete zooids per mm² in outer exozone T

ACANTHOSTYLE CHARACTERS (counted between maculae)

55. Number of complete acanthostyles per mm² in outer exozone T

APPENDIX 2

*Character state matrix of the multistate characters. Character numbers and states refer to Appendix 1. * designates outgroup species.*

| | Character no. |
|---|---|
| | 1111111111222222222233333333334 |
| | 1234567890123456789012345678901234567890 |
| *Bimuropora dubia* | 52322222212242165422232323333323523215232 |
| *Bimuropora pollaphragmata* | 52312223212242165122232313333323523215332 |
| *Bimuropora conferta* | 52332222212242165122232323333323523215432 |
| *Bimuropora winchelli* | 52332222212242165122232313333323523215232 |
| *Champlainopora chazyensis* | 52312112212211165222232313333311123215111 |
| *Champlainopora ramusculus* | 52312112212211125122232323333311123215111 |
| *Champlainopora pachymura* | 52312112212242165123232323334235232151111 |
| *Champlainopora arbucklensis* | 52332112212242165122232323333323523215332 |
| **Eridotrypa* sp. | 52211111112211124222242222333311123215242 |
| **Eridotrypa mutabilis* | 52211111112222124222242222333235232152 42 |

APPENDIX 3

*List of synapomorphic character states for Figure 5. Letters refer to that figure. Numbers refer to characters and states listed in Appendix 1.*

| | Character | State |
|---|---|---|
| A: | 1—Zoarial growth habit | 5—Ramose |
| | 2—Intracolony overgrowths | 2—Present |
| | 4—Surface angle | 1—0–70° |
| | 6—Zooidal arrangement | 1—Ordered |
| | 7—Large, long, axial zooecia | 1—Present |
| | 10—Remnant growing tips in endozone | 1—Present |
| | 11—Lines of distally concave diaphragms | 2—Present |
| | 12—Lines of diaphragms across endozone | 2—Present |
| | 13—Macular topography | 1—Maculae absent |
| | 14—Macular shape | 1—Maculae absent |
| | 15—Ontogenetic trend in autozooid living chamber shape | 1—Polygonal to subpolygonal |
| | 16—Autozooid living chamber cross-sectional shape in exozone | 2—Oval |
| | 18—Autozooid wall shape in endozone | 2—Wavy |
| | 19—Autozooid wall structure in exozone | 2—Integrate |
| | 20—Autozooid wall boundary shape in exozone | 2—Irregular |
| | 21—Autozooid wall laminae configuration | 2—Convex distally |
| | 23—Distally concave diaphragms | 2—Rare |
| | 25—S-shaped diaphragms | 2—Rare |
| | 27—Diaphragm insertion angle | 3—Variable |
| | 28—More distal side of basal diaphragms | 3—On distal side of zooid |
| | 29—Autozooid wall thickened by diaphragm | 3—On both sides of zooid |
| | 30—Megazooids | 1—Absent |
| | 31—Location of origination of megazooids | 1—Megazooids absent |
| | 32—Megazooid living chamber cross-sectional shape in exozone | 1—Megazooids absent |
| | 33—Distribution of mesozooids | 2—Only in corners of autozooids |
| | 34—Location of origination of mesozooids | 3—Endozone/exozone boundary |
| | 35—Mesozooid diaphragm shape | 2—Planar |
| | 36—Diaphragm insertion angle | 1—Roughly 90° |
| | 37—Mesozooidal boundary cross-sectional shape | 5—Polygonal |
| B: | 3—Branch cross-sectional shape | 2—Subcircular to oval |
| | 5—Type of interzooidal budding | 1—Intrazooidal pattern |
| | 8—Diaphragm spacing in early ontogeny | 1—0.0/mm |
| | 9—Length of mesozooidal stage in early ontogeny | 1—No mesozooidal stage in early ontogeny |
| | 17—Autozooidal boundary cross-sectional shape in exozone | 4—Subpolygonal |
| | 22—Planar diaphragms | 4—Abundant |
| | 24—Distally convex diaphragms | 2—Rare |
| | 26—Cystoidal diaphragms | 2—Rare |
| | 38—Distribution of acanthostyles | 2—Only in corners of adjacent autozooids |
| | 39—Location of origination of acanthostyles | 4—In exozone |
| | 40—Acanthostyle microstructure | 2—Distally convex laminae around core |
| C: | 13—Macular topography | 2—Flat |
| | 14—Macular shape | 2—Irregular |
| | 30—Megazooids | 2—Present |
| | 31—Location of origination of megazooids | 3—In outer endozone |
| | 32—Megazooid living chamber cross-sectional shape in exozone | 5—Subpolygonal |
| D: | 3—Branch cross-sectional shape | 3—Circular |
| | 5—Type of interzooidal budding | 2—Interzooidal pattern |
| | 8—Diaphragm spacing in early ontogeny | 2—0.1–9.0/mm |
| | 9—Length of mesozooidal stage in early ontogeny | 2—<0.1 mm |
| | 17—Autozooidal boundary cross-sectional shape in exozone | 5—Polygonal |

APPENDIX 3
*Continued.*

| | Character | State |
|---|---|---|
| | 22—Planar diaphragms | 3—Common |
| | 24—Distally convex diaphragms | 3—Common |
| | 26—Cystoidal diaphragms | 3—Common |
| | 38—Distribution of acanthostyles | 1—Absent |
| | 39—Location of origination of acanthostyles | 1—Acanthostyles absent |
| | 40—Acanthostyle microstructure | 1—Acanthostyles absent |
| E: | 16—Autozooid living chamber cross-sectional shape in exozone | 6—Subpolygonal |
| | 25—S-shaped diaphragms | 1—Absent |
| F: | 18—Autozooid wall shape in endozone | 1—Regular |
| G: | 13—Macular topography | 4—Elevated |
| | 14—Macular shape | 2—Irregular |
| | 16—Autozooid living chamber cross-sectional shape in exozone | 6—Subpolygonal |
| | 18—Autozooid wall shape in endozone | 1—Regular |
| | 20—Autozooid wall boundary shape in exozone | 3—Straight |
| | 29—Autozooid wall thickened by diaphragm | 4—Usually on distal side of zooid |
| | 30—Megazooids | 2—Present |
| | 31—Location of origination of megazooids | 3—In outer endozone |
| | 32—Megazooid living chamber cross-sectional shape in exozone | 5—Subpolygonal |
| H: | 4—Surface angle | 3—79–90° |
| | 13—Macular topography | 4—Elevated |
| | 14—Macular shape | 2—Irregular |
| | 16—Autozooid living chamber cross-sectional shape in exozone | 6—Subpolygonal |
| | 18—Autozooid wall shape in endozone | 1—Regular |
| | 30—Megazooids | 2—Present |
| | 31—Location of origination of megazooids | 3—In outer endozone |
| | 32—Megazooid living chamber cross-sectional shape in exozone | 5—Subpolygonal |
| | 38—Distribution of acanthostyles | 3—Surround zooids but do not inflect walls |
| | 39—Location of origination of acanthostyles | 3—Endozone/exozone boundary |
| | 40—Acanthostyle microstructure | 2—Distally convex laminae around core |
| I: | 6—Zooidal arrangement | 2—Disordered |
| | 7—Large, long, axial zooecia | 2—Absent |
| J: | 4—Surface angle | 2—71–78° |
| | 18—Autozooid wall shape in endozone | 4—Fluted |
| | 38—Distribution of acanthostyles | 2—Only in corners of adjacent autozooids |
| K: | 4—Surface angle | 1—0–70° |
| | 8—Diaphragm spacing in early ontogeny | 3—>9.0/mm |
| | 25—S-shaped diaphragms | 1—Absent |
| L: | 38—Distribution of acanthostyles | 4—Surround zooids and inflect walls |
| M: | 25—S-shaped diaphragms | 1—Absent |
| | 38—Distribution of acanthostyles | 2—Only in corners of adjacent autozooids |

APPENDIX 4

*List of synapomorphic character states for Figure 6. Letters refer to that figure. Numbers refer to characters and states listed in Appendix 1.*

| | Character | State |
|---|---|---|
| A: | 6—Zooidal arrangement | 1—Ordered |
| | 7—Large, long, axial zooecia | 1—Present |
| | 10—Remnant growing tips in endozone | 1—Present |
| B: | 5—Type of interzooidal budding | 1—Intrazooidal pattern |
| | 8—Diaphragm spacing in early ontogeny | 1—0.0/mm |
| | 9—Length of mesozooidal stage in early ontogeny | 1—No mesozooidal stage in early ontogeny |
| C: | 5—Type of interzooidal budding | 2—Interzooidal pattern |
| | 8—Diaphragm spacing in early ontogeny | 2—0.1–9.0/mm |
| | 9—Length of mesozooidal stage in early ontogeny | 2—<0.1 mm |
| D: | 6—Zooidal arrangement | 2—Disordered |
| | 7—Large, long, axial zooecia | 2—Absent |
| E: | 8—Diaphragm spacing in early ontogeny | 3—>9.0/mm |

APPENDIX 5

*Summary quantitative data for the Simpson Group colonies of Bimuropora dubia* (Loeblich). This includes Loeblich's holotype of *Hallopora dubia* (USNM 100497) and the hypotypes (USNM 435394–435405). See Appendix 1 for full character descriptions. All measurements in mm except where indicated.

| Character | Number of colonies | Minimum | Maximum | Mean | Standard deviation |
|---|---|---|---|---|---|
| 41—Surface angle (degrees) | 13 | 58.0 | 87.8 | 75.4 | 8.5 |
| 42—Endozone diameter | 13 | 2.26 | 5.38 | 3.53 | 0.95 |
| 43—Exozone width | 13 | 0.47 | 0.80 | 0.64 | 0.10 |
| 44—Branch diameter | 13 | 3.62 | 6.68 | 4.80 | 0.96 |
| 45—Axial ratio | 13 | 0.62 | 0.85 | 0.73 | 0.06 |
| 46—Living chamber area | 7 | 0.030 | 0.041 | 0.035 | 0.004 |
| 47—Living chamber diameter | 7 | 0.195 | 0.229 | 0.210 | 0.013 |
| 48—Living chamber depth | 10 | 0.244 | 0.400 | 0.333 | 0.058 |
| 49—Wall thickness | 13 | 0.041 | 0.06 | 0.050 | 0.006 |
| 50—Diaphragms per mm in bud | 13 | 6.0 | 11.2 | 8.7 | 1.4 |
| 51—Diaphragms per mm in endozone | 13 | 0.4 | 3.0 | 1.1 | 0.7 |
| 52—Diaphragms per mm in exozone | 13 | 4.4 | 13.0 | 7.5 | 2.5 |
| 53—Mesozooidal diaphragms per mm | 8 | 12.0 | 17.2 | 15.6 | 2.0 |
| 54—Mesozooids per mm² | 6 | 1.3 | 5.5 | 3.2 | 1.6 |
| 55—Acanthostyles per mm² | 4 | 9.0 | 16.0 | 13.4 | 3.3 |

APPENDIX 6

*Summary quantitative data for the Simpson Group colonies of Bimuropora pollaphragmata* n. gen. and sp. This includes the holotype (USNM 435406) and paratypes (USNM 435407–435419). See Appendix 1 for full character descriptions. All measurements in mm except where indicated.

| Character | Number of colonies | Minimum | Maximum | Mean | Standard deviation |
|---|---|---|---|---|---|
| 41—Surface angle (degrees) | 12 | 56.1 | 77.3 | 66.7 | 7.2 |
| 42—Endozone diameter | 13 | 1.68 | 3.98 | 2.82 | 0.68 |
| 43—Exozone width | 13 | 0.28 | 0.64 | 0.46 | 0.11 |
| 44—Branch diameter | 13 | 2.38 | 5.25 | 3.74 | 0.79 |
| 45—Axial ratio | 13 | 0.67 | 0.85 | 0.75 | 0.06 |
| 46—Living chamber area | 8 | 0.017 | 0.028 | 0.023 | 0.004 |
| 47—Living chamber diameter | 8 | 0.147 | 0.189 | 0.171 | 0.016 |
| 48—Living chamber depth | 12 | 0.205 | 0.330 | 0.278 | 0.041 |
| 49—Wall thickness | 14 | 0.031 | 0.079 | 0.050 | 0.013 |
| 50—Diaphragms per mm in bud | 12 | 9.0 | 11.0 | 10.0 | 0.6 |
| 51—Diaphragms per mm in endozone | 12 | 3.5 | 5.5 | 4.4 | 0.7 |
| 52—Diaphragms per mm in exozone | 12 | 7.1 | 18.1 | 10.4 | 3.8 |
| 53—Mesozooidal diaphragms per mm | 11 | 14.0 | 20.0 | 17.2 | 2.0 |
| 54—Mesozooids per mm² | 4 | 4.0 | 16.5 | 7.6 | 5.9 |
| 55—Acanthostyles per mm² | 2 | 5.5 | 43.3 | 24.4 | 26.7 |

APPENDIX 7

*Summary quantitative data for the Simpson Group colonies of Bimuropora conferta* (Coryell). This includes the hypotypes (USNM 435420–435431). See Appendix 1 for full character descriptions. All measurements in mm except where indicated.

| Character | Number of colonies | Minimum | Maximum | Mean | Standard deviation |
|---|---|---|---|---|---|
| 41—Surface angle (degrees) | 12 | 66.8 | 86.8 | 78.6 | 5.3 |
| 42—Endozone diameter | 12 | 2.28 | 3.64 | 3.02 | 0.44 |
| 43—Exozone width | 12 | 0.38 | 1.28 | 0.71 | 0.26 |
| 44—Branch diameter | 12 | 3.64 | 5.80 | 4.44 | 0.72 |
| 45—Axial ratio | 12 | 0.55 | 0.81 | 0.69 | 0.08 |
| 46—Living chamber area | 8 | 0.030 | 0.070 | 0.052 | 0.011 |
| 47—Living chamber diameter | 8 | 0.195 | 0.299 | 0.255 | 0.029 |
| 48—Living chamber depth | 12 | 0.268 | 0.359 | 0.318 | 0.029 |
| 49—Wall thickness | 12 | 0.033 | 0.067 | 0.044 | 0.010 |
| 50—Diaphragms per mm in bud | 10 | 5.4 | 8.8 | 7.2 | 1.0 |
| 51—Diaphragms per mm in endozone | 11 | 0.1 | 1.3 | 0.5 | 0.4 |
| 52—Diaphragms per mm in exozone | 12 | 3.5 | 11.9 | 5.9 | 2.3 |
| 53—Mesozooidal diaphragms per mm | 7 | 12.0 | 16.4 | 14.2 | 1.8 |
| 54—Mesozooids per mm² | 3 | 1.5 | 7.0 | 4.0 | 2.8 |
| 55—Acanthostyles per mm² | 3 | 16.0 | 22.3 | 18.4 | 3.4 |

APPENDIX 8

*Summary quantitative data for the Simpson Group colonies of Bimuropora winchelli* (Ulrich). This includes Loeblich's holotype (USNM 114566) of *Batostoma chapparsi*, Loeblich's hypotype (USNM 114572) of *Amplexopora winchelli*, and the hypotypes (USNM 435436–435447). See Appendix 1 for full character descriptions. All measurements in mm except where indicated.

| Character | Number of colonies | Minimum | Maximum | Mean | Standard deviation |
|---|---|---|---|---|---|
| 41—Surface angle (degrees) | 12 | 65.4 | 88.3 | 78.6 | 7.7 |
| 42—Endozone diameter | 12 | 1.74 | 4.92 | 3.31 | 0.96 |
| 43—Exozone width | 12 | 0.48 | 1.32 | 0.83 | 0.31 |
| 44—Branch diameter | 12 | 3.17 | 7.48 | 4.96 | 1.26 |
| 45—Axial ratio | 12 | 0.51 | 0.80 | 0.67 | 0.09 |
| 46—Living chamber area | 12 | 0.032 | 0.055 | 0.042 | 0.007 |
| 47—Living chamber diameter | 12 | 0.202 | 0.265 | 0.229 | 0.020 |
| 48—Living chamber depth | 11 | 0.260 | 0.445 | 0.318 | 0.059 |
| 49—Wall thickness | 14 | 0.036 | 0.079 | 0.051 | 0.012 |
| 50—Diaphragms per mm in bud | 13 | 5.2 | 10.0 | 8.0 | 1.3 |
| 51—Diaphragms per mm in endozone | 14 | 0.6 | 3.4 | 1.4 | 0.8 |
| 52—Diaphragms per mm in exozone | 12 | 3.7 | 13.2 | 8.3 | 2.5 |
| 53—Mesozooidal diaphragms per mm | 11 | 11.0 | 18.0 | 15.2 | 2.1 |
| 54—Mesozooids per mm² | 8 | 1.5 | 3.0 | 2.4 | 0.7 |
| 55—Acanthostyles per mm² | 8 | 19.0 | 27.0 | 23.7 | 2.8 |

APPENDIX 9

*Summary quantitative data for the Simpson Group colonies of Champlainopora chazyensis* (Ross). This includes the hypotypes (USNM 435448–435467). See Appendix 1 for full character descriptions. All measurements in mm except where indicated.

| Character | Number of colonies | Minimum | Maximum | Mean | Standard deviation |
|---|---|---|---|---|---|
| 41—Surface angle (degrees) | 19 | 49.0 | 77.9 | 62.6 | 7.9 |
| 42—Endozone diameter | 19 | 0.84 | 2.52 | 1.45 | 0.42 |
| 43—Exozone width | 19 | 0.29 | 0.68 | 0.48 | 0.11 |
| 44—Branch diameter | 19 | 1.48 | 3.24 | 2.41 | 0.49 |
| 45—Axial ratio | 19 | 0.49 | 0.78 | 0.60 | 0.08 |
| 46—Living chamber area | 19 | 0.010 | 0.035 | 0.021 | 0.008 |
| 47—Living chamber diameter | 19 | 0.113 | 0.211 | 0.159 | 0.033 |
| 48—Living chamber depth | 18 | 0.188 | 0.428 | 0.291 | 0.075 |
| 49—Wall thickness | 20 | 0.065 | 0.159 | 0.113 | 0.021 |
| 50—Diaphragms per mm in bud | 14 | 7.3 | 12.0 | 9.3 | 1.3 |
| 51—Diaphragms per mm in endozone | 17 | 0.9 | 6.8 | 2.7 | 1.5 |
| 52—Diaphragms per mm in exozone | 19 | 4.2 | 19.4 | 9.8 | 3.9 |
| 53—Mesozooidal diaphragms per mm | 8 | 14.0 | 20.0 | 17.7 | 2.0 |
| 54—Mesozooids per mm² | 17 | 0.6 | 6.0 | 3.0 | 1.3 |
| 55—Acanthostyles per mm² | 20 | 0.0 | 0.0 | 0.0 | 0.0 |

APPENDIX 10

*Summary quantitative data for the Simpson Group colonies of Champlainopora ramusculus* n. sp. This includes the holotype (USNM 435468) and paratypes (USNM 435469–435481). See Appendix 1 for full character descriptions. All measurements in mm except where indicated.

| Character | Number of colonies | Minimum | Maximum | Mean | Standard deviation |
|---|---|---|---|---|---|
| 41—Surface angle (degrees) | 14 | 48.4 | 67.2 | 60.3 | 6.0 |
| 42—Endozone diameter | 14 | 0.68 | 1.62 | 1.02 | 0.23 |
| 43—Exozone width | 14 | 0.26 | 0.44 | 0.33 | 0.05 |
| 44—Branch diameter | 14 | 1.38 | 2.36 | 1.67 | 0.27 |
| 45—Axial ratio | 14 | 0.49 | 0.70 | 0.60 | 0.06 |
| 46—Living chamber area | 10 | 0.018 | 0.035 | 0.025 | 0.006 |
| 47—Living chamber diameter | 10 | 0.151 | 0.211 | 0.178 | 0.020 |
| 48—Living chamber depth | 9 | 0.167 | 0.340 | 0.269 | 0.049 |
| 49—Wall thickness | 14 | 0.059 | 0.120 | 0.079 | 0.020 |
| 50—Diaphragms per mm in bud | 12 | 6.0 | 13.3 | 9.3 | 2.3 |
| 51—Diaphragms per mm in endozone | 14 | 0.3 | 6.0 | 2.4 | 1.7 |
| 52—Diaphragms per mm in exozone | 14 | 4.2 | 24.2 | 12.0 | 6.0 |
| 53—Mesozooidal diaphragms per mm | 9 | 13.0 | 24.0 | 19.1 | 3.4 |
| 54—Mesozooids per mm² | 9 | 2.5 | 14.0 | 7.5 | 4.0 |
| 55—Acanthostyles per mm² | 14 | 0.0 | 0.0 | 0.0 | 0.0 |

APPENDIX 11

*Summary quantitative data for the Simpson Group colonies of Champlainopora pachymura* (Loeblich). This includes Loeblich's holotype (USNM 114604) and paratype (USNM 100482) of *Hallopora pachymura* and the hypotypes (USNM 435482–435496). See Appendix 1 for full character descriptions. All measurements in mm except where indicated.

| Character | Number of colonies | Minimum | Maximum | Mean | Standard deviation |
|---|---|---|---|---|---|
| 41—Surface angle (degrees) | 17 | 51.0 | 80.1 | 69.6 | 6.5 |
| 42—Endozone diameter | 17 | 2.13 | 3.42 | 2.60 | 0.38 |
| 43—Exozone width | 17 | 0.40 | 0.95 | 0.65 | 0.16 |
| 44—Branch diameter | 17 | 3.36 | 4.62 | 3.90 | 0.43 |
| 45—Axial ratio | 17 | 0.58 | 0.79 | 0.67 | 0.07 |
| 46—Living chamber area | 17 | 0.030 | 0.071 | 0.045 | 0.010 |
| 47—Living chamber diameter | 17 | 0.195 | 0.301 | 0.239 | 0.026 |
| 48—Living chamber depth | 12 | 0.196 | 0.399 | 0.300 | 0.065 |
| 49—Wall thickness | 17 | 0.057 | 0.120 | 0.081 | 0.020 |
| 50—Diaphragms per mm in bud | 15 | 6.5 | 11.0 | 9.1 | 1.6 |
| 51—Diaphragms per mm in endozone | 16 | 0.4 | 4.3 | 2.4 | 1.2 |
| 52—Diaphragms per mm in exozone | 17 | 5.0 | 15.7 | 9.6 | 3.0 |
| 53—Mesozooidal diaphragms per mm | 7 | 12.0 | 22.0 | 17.7 | 3.1 |
| 54—Mesozooids per mm² | 16 | 0.0 | 8.0 | 2.4 | 2.2 |
| 55—Acanthostyles per mm² | 17 | 0.0 | 0.0 | 0.0 | 0.0 |

APPENDIX 12

*Summary quantitative data for the Simpson Group colonies of Champlainopora arbucklensis* n. sp. This includes the holotype (USNM 435497) and paratypes (USNM 435498–435512). See Appendix 1 for full character descriptions. All measurements in mm except where indicated.

| Character | Number of colonies | Minimum | Maximum | Mean | Standard deviation |
|---|---|---|---|---|---|
| 41—Surface angle (degrees) | 15 | 72.5 | 86.4 | 83.5 | 3.5 |
| 42—Endozone diameter | 15 | 1.84 | 3.10 | 2.38 | 0.35 |
| 43—Exozone width | 15 | 0.47 | 2.08 | 1.15 | 0.43 |
| 44—Branch diameter | 15 | 3.50 | 6.50 | 4.67 | 0.74 |
| 45—Axial ratio | 15 | 0.36 | 0.77 | 0.52 | 0.12 |
| 46—Living chamber area | 13 | 0.014 | 0.043 | 0.024 | 0.008 |
| 47—Living chamber diameter | 13 | 0.134 | 0.234 | 0.173 | 0.026 |
| 48—Living chamber depth | 12 | 0.274 | 0.478 | 0.391 | 0.061 |
| 49—Wall thickness | 16 | 0.072 | 0.166 | 0.102 | 0.023 |
| 50—Diaphragms per mm in bud | 15 | 6.0 | 11.8 | 9.2 | 1.5 |
| 51—Diaphragms per mm in endozone | 15 | 0.8 | 4.0 | 2.3 | 0.8 |
| 52—Diaphragms per mm in exozone | 15 | 5.3 | 12.0 | 8.5 | 2.0 |
| 53—Mesozooidal diaphragms per mm | 11 | 14.7 | 19.3 | 17.3 | 1.6 |
| 54—Mesozooids per mm² | 13 | 0.4 | 3.0 | 1.7 | 0.6 |
| 55—Acanthostyles per mm² | 13 | 20.5 | 35.4 | 26.2 | 4.2 |